Novel lectin-based chimeric antigen receptors target Gb3-positive tumour cells

Winfried Römer (winfried.roemer@bioss.uni-freiburg.de)
University of Freiburg im Breisgau: Albert-Ludwigs-Universitat Freiburg https://orcid.org/0000-0002-2847-246X

Ana Valeria Meléndez
University of Freiburg im Breisgau: Albert-Ludwigs-Universitat Freiburg

Rubí M-H Velasco Cárdenas
University of Freiburg im Breisgau: Albert-Ludwigs-Universitat Freiburg

Simon Lagies
University of Freiburg im Breisgau: Albert-Ludwigs-Universitat Freiburg

Lina Siukstaite
University of Freiburg im Breisgau: Albert-Ludwigs-Universitat Freiburg

Oliver S. Thomas
University of Freiburg im Breisgau: Albert-Ludwigs-Universitat Freiburg

Wilfried Weber
University of Freiburg im Breisgau: Albert-Ludwigs-Universitat Freiburg

Bernd Kammerer
University of Freiburg im Breisgau: Albert-Ludwigs-Universitat Freiburg

Susana Minguet
University of Freiburg im Breisgau: Albert-Ludwigs-Universitat Freiburg

Research Article

Keywords: Lectin , CAR T-cells , Cancer , Tumour-associated carbohydrate antigens , Glycosphingolipid targeting , Globotriaosylceramide

Posted Date: April 27th, 2022

DOI: https://doi.org/10.21203/rs.3.rs-1327761/v1

Novel lectin-based chimeric antigen receptors target Gb3-positive tumour cells

Ana Valeria Meléndez[1,2,3,4], Rubí M-H Velasco Cárdenas[1,2,3], Simon Lagies[5], Lina Siukstaite[1,2,3], Oliver S. Thomas[1,2,3,4] Wilfried Weber[1,2,3,4], Bernd Kammerer[2,5,6], Winfried Römer[1,2,3,4,7,*] and Susana Minguet[1,2,3,4,7,8,*]

[1] Faculty of Biology, University of Freiburg, Schänzlestraße 1, 79104 Freiburg, Germany

[2] BIOSS, Centre for Biological Signalling Studies, University of Freiburg, Schänzlestraße 18, 79104 Freiburg, Germany

[3] CIBSS, Centre for Integrative Biological Signalling Studies, University of Freiburg, Schänzlestraße 18, 79104 Freiburg, Germany

[4] Spemann Graduate School of Biology and Medicine (SGBM), University of Freiburg, Albertstraße 19a, 79104 Freiburg, Germany

[5] Institute of Organic Chemistry, Albert-Ludwigs-University Freiburg, Albertstraße 21, 79102 Freiburg, Germany

[6] Centre for Integrative Signalling Analysis, University of Freiburg, Habsburgerstraße 49, 79104 Freiburg, Germany

[7] Freiburg Institute for Advanced Studies (FRIAS), University of Freiburg, Freiburg, Germany

[8] Center of Chronic Immunodeficiency (CCI), University Clinics and Medical Faculty, Freiburg, Germany

*corresponding authors

To whom correspondence should be addressed:

Prof. Dr. Winfried Römer, winfried.roemer@bioss.uni-freiburg.de

PD Dr. Susana Minguet, susana.minguet@biologie.uni-freiburg.de

ORCID iDs: 0000-0001-6267-2855 (Ana Valeria Meléndez), 0000-0002-1764-115X (Rubí M-H Velasco Cárdenas), 0000-0002-5245-1781 (Simon Lagies), 0000-0002-0899-1916 (Lina Siukstaite), 0000-0003-1949-0938 (Oliver S. Thomas), 0000-0003-4340-4446 (Wilfried Weber), 0000-0002-2847-246X (Winfried Römer), 0000-0001-8211-5538 (Susana Minguet).

Abstract

A link between cancer and aberrant glycosylation has recently become evident. Glycans and their altered forms, known as tumour-associated carbohydrate antigens (TACAs), are diverse, complex and difficult to target therapeutically. Lectins are naturally occurring glycan-binding proteins and offer a unique opportunity to recognise TACAs. T cells expressing chimeric antigen receptors (CARs) have proven to be a successful immunotherapy against leukaemias, but so far have shown limited success in solid tumours. We developed a panel of lectin-CARs that recognise the glycosphingolipid globotriaosylceramide (Gb3), which is overexpressed in various cancers, such as Burkitt's lymphoma, colorectal, breast and pancreatic cancer. We have selected the following lectins: Shiga toxin's B-subunit from *Shigella dysenteriae*, LecA from *Pseudomonas aeruginosa*, and the engineered lectin Mitsuba from *Mytilus galloprovincialis* as antigen-binding domains and fused them to a well-known second generation CAR. The Gb3-binding lectin-CARs have demonstrated target-specific cytotoxicity against Burkitt's lymphoma-derived cell lines as well as solid tumour cells from colorectal and triple negative breast cancer. Our findings reveal the big potential of lectin-based CARs as therapeutical applications to target Gb3 and other TACAs expressed in haematological malignancies and solid tumours.

Keywords

Lectin · CAR T-cells · Cancer · Tumour-associated carbohydrate antigens · Glycosphingolipid targeting · Globotriaosylceramide

Abbreviations

BLI	Bioluminescence
CAR	Chimeric antigen receptors
DMEM	Dulbecco's Modified Eagle Medium
DOPC	1,2-dioleoyl-sn-glycero-3-phosphocholine

DOPE	1,2-dioleoyl-sn-glycero-3- phosphoethanolamine
ELISA	Enzyme-linked immunoabsorbent assay
E:T	Effector to target
PBS	Phosphate-buffered saline
Gb3	Globotriaosylceramide
GSL	Glycosphingolipid
GUV	Giant unilamellar vesicles
HBSS	Hanks' balanced salt solution
IFN-γ	Interferon γ
IMDM	Iscove's Modified Dulbecco's Medium
IS	Internal standard
ITO	Indium tin oxid-covered
LC	Liquid chromatography
MFI	Mean fluorescence intensity
MOI	Multiplicity of infection
MS	Mass spectrometry
NT	Non-transduced cells
NEAA	Non-essential amino acids
PBMC	Peripheral blood mononuclear cell
PPMP	1-phenyl-2-palmitoylamino-3-morpholino-1-propanol
RLU	Relative light units
RPMI	Roswell Park Memorial Institute
scFv	Single-chain variable fragment
SDS	Sodium dodecyl sulfate
StxB	Shiga toxin B-subunit
TACAs	Tumour-associated carbohydrate antigens
TNF-α	Tumour necrosis factor α

Introduction

The successful treatment of B-cell malignancies with chimeric antigen receptor (CAR) T cells has demonstrated the therapeutical potential of cell-based immunotherapies against cancer [1, 2]. CARs are engineered receptors that redirect and activate T cells upon encounter to a tumour-specific antigen to eventually eliminate cancer cells. CAR T cells combine an antigen-binding domain, traditionally a single-chain variable fragment (scFv), with a transmembrane domain and an intracellular signalling domain [3]. To date, CAR T cells primarily use scFv derived from antibodies targeting cell surface proteins, such as CD19 on B lymphocytes. However, one of the main mechanisms to overcome CAR recognition of cell surface proteins is antigen escape, which leads to recurrence after treatment [4, 5].

In addition to surface proteins and receptors, glycans can be found on the cell surface. Cell surface glycans participate in critical cellular processes such as cell-cell communication and disease development and progression. Given the importance of glycosylation, it is not surprising that minor changes in this process profoundly impact cell biology [6]. The dysregulation of the glycan biosynthetic pathway is reflected as aberrant glycosylation and leads to malignant transformation [7, 8]. Altered glycan profiles include the appearance of truncated or novel structures, accumulation of precursors, and loss or overexpression of specific glycan structures on cancer cell surfaces named tumour-associated carbohydrate antigens (TACAs)[9, 10]. Therefore, targeting glycans could be a broader and more effective anti-cancer strategy than targeting subjacent core proteins [11]. Glycan-binding proteins, namely antibodies and lectins, recognise altered glycan profiles in malignant cells might provide an instrumental basis for tumour-targeted immunotherapy [12, 13]. On the one hand, carbohydrate-binding antibodies have been investigated for several decades to target TACAs. However, only a few were approved for clinical use due to the wide variety of glycan epitopes and reduced antibody recognition [10, 14, 15]. On the other hand, lectins are proteins that recognise and bind carbohydrate moieties present in lipids and proteins, valuable tools in biotechnology and medicine. Lectins have been used for cancer diagnosis, imaging [16, 17], and are currently explored as drug delivery systems [18–20]. Thus, lectins represent a promising addition to antibody-based applications. Most TACAs, particularly glycosphingolipids (GSLs) are poor immunogens [21]. Therefore, it is not easy to generate high affinity antibodies that could be applied in immunotherapy. For this reason, novel non-antibody-based approaches should be developed to target TACAs.

Most human cancers exhibit alterations in GSLs composition and metabolism, including those from the globo-series. The association of GSLs with cancer was first reported more than 50 years ago [22]. Among the globo-series, the globotriaosylceramide (Gb3, also known as CD77 or P^k antigen) [23, 24] was first identified as a fibrosarcoma-associated antigen [25]. Gb3 is present in the extracellular leaflet of the plasma membrane [26, 27]. It is composed of a ceramide backbone linked to a neutral trisaccharide made of galactose (Gal) and glucose (Glc) (Galα1-4Galβ1-4Glc) [24, 28]. The ceramide consists of sphingosine and a fatty acyl chain with different lengths, degrees of saturation and hydroxylation [27, 29, 30]. Gb3 is highly expressed in Burkitt's lymphoma [31], colorectal carcinoma [32], breast [33], ovary, and pancreatic cancer [34], as well as gliomas [35] and acute non-lymphocytic leukaemia (ANLL) [36]. Furthermore, Gb3 has been correlated with invasiveness, metastasis, angiogenesis and multi-drug resistance [37–41]. Overall, Gb3 might be an attractive target for engineering CAR T cells. Indeed, numerous lectins from unique origins have specificity for Gb3 [42], such as LecA from *Pseudomonas aeruginosa* [43], the non-toxic B-subunit of Shiga toxin (StxB), produced by

Shigella dysenteriae and enterohemorrhagic strains of *Escherichia coli* (EHEC) [44], and the computationally redesigned Mitsuba [45] from the shellfish lectin MytiLec-1 [46].

In the present study, we successfully generated a panel of CARs, each of them with a Gb3-binding lectin as antigen-binding domain linked to the intracellular signalling domains from 41BB and CD3ζ. Lectins with different molecular weights and architectures but a common specificity towards Gb3 were chosen. *In vitro* analyses revealed that lectin-CAR T cells specifically recognised $Gb3^+$ cancer cells and were cytotoxically active against cell lines from Burkitt's lymphoma, colorectal and breast cancer.

Material and Methods

Cell lines

Ramos, Raji and Namalwa cells were grown in Roswell Park Memorial Institute (RPMI) 1640 medium. HT-29, HCT-116, LS-174 cells were cultured in Dulbecco's Modified Eagle Medium (DMEM) with 4.5 gL^{-1} glucose. MDA-MB-231 and JIMT1 cells were grown in DMEM with 1 gL^{-1} glucose. All media were supplemented with 10% fetal calf serum (FCS) and antibiotics; the cells were cultured at 37°C and 5% CO_2. Daudi cells were grown in Iscove's Modified Dulbecco's Medium (IMDM) and HEK293T cells in DMEM, both media supplemented with 10% fetal bovine serum and antibiotics; cells were cultured at 37°C and 7.5% CO_2.

Antibodies

The following antibodies were applied for activation: anti-CD28.2 (BioLegend #302902), anti-mouse CD3ε (145-2C11, here named 2C11, from J. Bluestone, San Francisco, CA, USA). An anti-ζ antiserum 449 and a secondary antibody anti-mouse were used for immunoblotting. The following antibodies were utilised for flow cytometry: APC-labeled anti-FLAG (#637307), Alexa Fluor 488-labelled anti-CD3 (#300415), PE-labeled anti-hCD25 (#302606) all from BioLegend. APC-labelled anti-hCD69 (#MHCD6905) from Invitrogen, APC-labeled anti-hCD8 (#IM2469) from Beckman Coulter and PE-Cy7-labeled anti-CD137 (#25-1371-82) from eBioscience.

Generation of CAR constructs

To generate CARs targeting Gb3, the sequences encoding the B-subunit of Shiga toxin (StxB) from *S. dysenteriae*, LecA from *P. aeruginosa,* and Mitsuba, a variant of the shellfish lectin MytiLec-1, were cloned in frame with the lentiviral vector pCDH-EF1-19BBζ-T2A-copGFP. The lectin amino acid sequences were obtained from Uniprot or PDB and the synthesised gene from Integrated DNA Technologies. The lentiviral vector was a gift from TCR2 Therapeutics. This second-generation CAR consists of the scFv from murine anti-hCD19 (FMC63) fused to the extracellular and transmembrane region of human CD8α, the 41BB endodomain and the ζ cytoplasmic tail signalling domain under the control of an EF-1α promoter. The sequence of each cloned CAR was verified via sequencing.

Lentivirus production and lentiviral transduction

A total of 10^7 HEK293T cells were plated and incubated overnight. After medium exchange, the HEK293T cells were transfected with the packaging plasmid pMD2.G, the gag/pol pCMVR8.74 and the respective construct using PEI (Polysciences) transfection. The medium containing lentiviral particles was collected at 24 and 48 h post-transfection

and concentrated by a 10% sucrose gradient. After 4 h of centrifugation at 10 000 rpm and 6°C, the supernatant was discarded, and the virus pellet was resuspended in phosphate-buffered saline (PBS) to be stored at -80°C.

Activation of primary human T cells, transduction and expansion

Peripheral blood mononuclear cells (PBMCs) were isolated from fresh blood of healthy donors using density centrifugation (Pancoll). PBMCs were resuspended in RPMI medium with 1000 Uml^{-1} of recombinant IL-2 (Prepotech) and activated with anti-CD3/CD28 (1 $mgml^{-1}$) antibodies. After 48-72 h, the remaining cells, mostly T cells, were lentivirally transduced using spin transfection (1800 rpm for 90 min and 30°C) in the presence of 5 mg ml^{-1} protamine sulfate (Sigma) and 1000 Uml^{-1} IL-2 with a multiplicity of infection (MOI) of 4. Cells were maintained in medium supplemented with 100 Uml^{-1} IL-2 for a maximum of 6-7 days after transduction before use for indicated experiments. Activated but non-lentiviral transduced cells (NT) were included as a control.

CAR expression

Transduced efficiency was monitored by BFP expression after 4-6 days. The CAR surface expression was verified with anti-FLAG antibody by flow cytometry. Samples were analysed using a GALLIOS flow cytometer (Beckman Coulter), and data analysis was performed using FlowJo V.10. The presence of the CARs after transduction was also confirmed by immunoblotting. A total of $5x10^5$ transduced cells were resuspended in 20 μl of 200 mM Tris. The samples were split into two equal parts, and cells were lysed either with reducing sodium dodecyl sulfate (SDS) buffer or non-reducing buffer plus 5 μl of urea. The samples were boiled for 5 min at 95 °C. Then the proteins were separated on 8% Tris-glycine gels and transferred on a nitrocellulose membrane. Primary antibody anti-ζ chain (1:1000) was added and incubated overnight at 4 °C. The corresponding horseradish peroxidase-conjugated secondary antibody (1:10000) was incubated with the membrane for an hour at room temperature (RT). Finally, ClarityTM Western ECL Chemiluminescent Substrate (Bio-Rad) was used to detect the luminescence signal by a Vilber Lourmat Fusion FX chemiluminescence imager.

Cytotoxicity assay

For the bioluminescence-based cytotoxicity assay, luciferase-expressing tumour cells (Ramos, Daudi, Raji, Namalwa, HT-29, HCT-116, LS-174, MDA-MB-231 or JIMT1, as indicated) were plated at a concentration of 10^4 cells ml^{-1} in 96-well flat bottom plates in triplicates. Then, 75 μgml^{-1} of D-firefly luciferin potassium salt (Biosynth) were added to the tumour cells, and bioluminescence (BLI) was measured in the luminometer (Tecan infinity M200 Pro) to establish the BLI baseline. Subsequently, CAR T cells were added in a 5:1 effector to target (E:T) ratio and incubated for 12, 17, 24 or 48 h (as indicated) at 37 °C. BLI was measured as relative light units (RLUs). RLU signals from cells treated with 1% Triton X-100 indicate maximal cell death. RLU signals from tumour cells incubated with non transduced T cells determine baseline cell death. Percent specific lysis (specific killing) was calculated with the following formula: % specific lysis = 100 × (average baseline death RLU − test RLU) / (average baseline death RLU − average maximal death RLU).

Cytokine detection

Cytokine release was tested using a commercially available enzyme-linked immunoabsorbent assay (ELISA) kit for tumour necrosis factor α (TNF-α) and interferon γ (IFN-γ) (Invitrogen). ELISAs were conducted according to the manufacturer's instructions. All CAR T cells were co-cultured with Ramos or Namalwa cells to a 5:1 effector to target

(E:T) ratio for 48 h in triplicate wells. The supernatant was collected, and the TNF-α and IFN-γ concentrations were measured in a microplate reader (Synergy H4, Biotek Instruments).

Activation of CAR T cells

The activation of CAR T cells was assessed by co-culturing CAR T cells with target cells for 48 h to a 5:1 E:T ratio in triplicate wells**.** T cells were stained with anti-CD3, anti-CD25, anti-CD8 and anti-CD137 antibodies. Samples were analysed using the Attune NxT flow cytometer (Thermo Fisher), and data analysis was performed using FlowJo V.10.

Gb3 inhibition by PPMP treatment

Ramos cells, $2x10^5$ cells per well, were seeded into a six-well plate and exposed to 1 and 2 µM of 1-phenyl-2-palmitoylamino-3-morpholino-1-propanol (PPMP from Enzo Life Sciences) for 48 h. At this time point, cells were washed with PBS, and fresh PPMP was added. After 24 h, to detect Gb3, the cells were stained with labelled StxB (Sigma Aldrich) and analysed using the GALLIOS flow cytometer. The data were analysed using FLowJo V.10. To verify cell viability after PPMP treatment, we used a cell proliferation and viability kit (Millipore Sigma) and followed the manufacturer's instructions. $1x10^4$ Ramos cells were seeded and supplemented with 10 µl of the MTT labelling reagent. After 4 h, 100 µl of solubilisation solution were added and incubated overnight at 37°C, 5% CO_2. Cell viability was measured at the microplate reader (Synergy HT, Biotek Instruments).

Gb3 profiling by LC/MS analysis

One day before the analysis, Ramos, Namalwa, HT-29, LS-174 and MDA-MB-231 cells were seeded in six-well plates. Gb3 composition analysis was done as described previously [47]. In brief, cells were washed with 0.9% NaCl and quenched with 1 ml methanol:water (1:1, v/v). Then, they were transferred to a new tube and lysed with 500 µl of a chloroform solution with 2 $\mu g ml^{-1}$ heptadecanoic acid by vigorous vortexing. 200 µl of the lower phase were evaporated and analysed by targeted LC-MS analysis. Chromatographic separation was achieved on a BEH-C18 column (Waters, 2.1x100 mm, 1.8 µm). It was used with A, a gradient acetonitrile:H_2O 6:4, 10 mM ammonium formate, 0.1% formic acid, and B, isopropanol:acetonitrile 9:1, 10 mM ammonium formate, 0.1% formic acid [48]. A triple quadrupole mass spectrometer (Agilent Technologies, G6460A) was operated in dynamic multiple reaction monitoring. Three experimental replicates were analysed in one LC-MS sequence. Samples were injected in randomised order, and a pooled quality control sample was regularly injected. Gb3 species were normalised to internal standard and peak sum of detected sphingolipids. MetaboAnalyst 5.0 [49] was used for visualisation. Data were range-scaled for the heat map.

Composition and preparation of Giant Unilamellar Vesicles

Giant unilamellar vesicles (GUVs) were composed of 1,2-dioleoyl-sn-glycero-3-phosphocholine (DOPC), cholesterol (both Avanti Polar Lipids) Atto 647N 1,2-dioleoyl-sn-glycero-3-phosphoethanolamine (DOPE, Sigma Aldrich), and Gb3 (Matreya) at a molar ratio of 59.7: 30: 0.3: 10 mol%, respectively. GUVs were prepared by the electroformation method described by Madl et al. 2016. Shortly, lipids dissolved in chloroform with a total concentration of 0.5 $mgmL^{-1}$ were spread on indium tin oxid-covered (ITO) glass slides and dried in a vacuum for at least one hour or overnight. Two ITO slides were assembled to make a chamber filled with sucrose solution adapted to the osmolarity of the imaging buffer Hanks' Balanced Salt Solution (HBSS, Thermo Fisher Scientific). Then, an alternating electrical field with a strength of 1 Vmm^{-1} was applied for 2.5 h at RT. Later, we observed the GUVs in chambers manually built as described [50].

Live-cell imaging

On the day of the experiment, BFP-sorted cells were stained with green CellTrace™CFSE proliferation kit (Thermo Fisher Scientific) following the manufacturer's instructions and rested in standard culture conditions, for at least 2 h, before starting the experiment. Cells were pre-washed with and kept in HBSS supplemented with 1% (v/v) FCS, 1 mM L-glutamine, 1% (v/v) non-essential amino acids (NEAA), 10 mM N-2-Hydroxyethylpiperazine-N'-2-ethanesulfonic Acid (HEPES), 0.55% (w/v) D-glucose while imaging. GUVs were added to the CAR T cell samples and imaged at 37°C using an incubator stage (Okolab) mounted onto a confocal laser scanning microscope (Nikon Eclipse Ti-E inverted microscope equipped with Nikon A1R confocal laser scanning system, 60x oil immersion objective, NA= 1.49, with three lasers: 488 nm, 561 nm, and 640 nm). Image acquisition and processing were performed using the NIS-Elements software (version 4.5, Nikon). The assembly of the videos (Online Resource 1-2) was done with Fiji Image J 2.1.0 software.

Image analysis

The captured time series were analysed for GUVs and CAR T cells contact. First, image segmentation was performed using ilastik [51], then GUVs, cells and co-localised pixels were quantified. The percent of contact between GUVs and cells was calculated using the following formula: % contact = 100 x (co-localised pixels) / (GUVs pixels + cells pixels). The percentage was estimated for each time point and monitored area.

Quantification and statistical analysis

Statistical parameters, including the exact value of *n*, precision measures (mean ± s.e.m. or median ± s.e.m) and statistical significance, are reported in figures and figure legends. Data were judged to be statistically significant when $p < 0.05$. In figures, asterisks denote statistical significance as calculated by one-way analysis of variance (ANOVA) or two-way ANOVA as indicated ($^{*}p < 0.05$; $^{**}p < 0.01$; $^{***}p < 0.001$; $^{****}p < 0.0001$; ns, not significant). Statistical analysis was performed in GraphPad Prism8.

Results

Engineered T cells express lectin-based CARs

Previous studies demonstrated that Gb3 is overexpressed in leukaemia, colorectal, breast, lung, ovarian, and testicular cancer, among other malignancies [39, 52]. We aimed here to target Gb3 in tumours by genetically engineered T cells since antibody-mediated targeting of glycosphingolipids appeared difficult [53]. We designed a novel group of lectin-based CARs. We introduced the sequences of Gb3-binding lectins into a well-characterised second-generation CAR [54]. These novel lectin-CARs have as antigen-binding domain the StxB from *S. dysenteriae*, the LecA from *P. aeruginosa* or Mitsuba, an engineered variant of MytiLec-1 from *M. galloprovincialis* [45]. Sequences encoding these Gb3-binding lectins were cloned in frame into a lentivirus vector to express a second-generation CAR including 41BB and CD3ζ as signalling domains and a fluorescence protein (blue fluorescent protein, BFP) to assay for transduction efficiencies. All CARs in this study share the same transmembrane and signalling domain and include a FLAG-tag for detection (Fig. 1a). As a control, a well-characterised anti-CD19-CAR was used in this study [54].

Activated human PBMCs were lentivirally transduced to express the different lectin-CARs (named Shiga-CAR, LecA-CAR and Mitsuba-CAR), the anti-CD19-CAR or an empty vector, indicated as mock. The transduction efficiency was

monitored by BFP expression, and the presence of the CARs on the cell surface was confirmed by FLAG-tag staining by flow cytometry. The BFP expression levels were similar in all cases, indicating similar transduction efficiencies. In contrast, CAR expression levels differed between CARs suggesting differences in folding or transport to the cell surface among the constructs or inaccessibility to the FLAG-tag. The frequency of cells expressing the CARs on the cell surface ranged from 36 to 85% (Fig. 1b-c). The FLAG-tag geometric mean fluorescence intensity (MFI) in CAR T cells revealed that the LecA-CAR had the highest T cell surface expression, followed by anti-CD19-CAR, Shiga-CAR and Mitsuba-CAR, among independent donors (Fig. 1b-d). We next confirmed the CAR expression by immunoblotting (Fig. S1a-b). All CARs exhibited the expected sizes under reducing conditions. In non-reducing gels, higher molecular weight complexes were observed. Despite identical cysteines located in the hinge and transmembrane regions of all CARs, each CAR construct presented a unique oligomerisation pattern (Fig. S1b). The LecA-CAR presented two clear bands that might correspond to a monomeric and tetrameric conformation, which is the native state of LecA. For the Shiga-CAR, two bands were detected, which correspond to that of a dimer or a trimer. The Mistuba-CAR exposed one band corresponding to a monomer. Finally, the anti-CD19-CAR revealed two bands: monomers and higher degree oligomers. Thus, the observed specific pattern of oligomerisation most probably results from the natural tendency of lectins to oligomerise [42].

Lectin-based CAR T cells mediate the lysis of tumour cells *in vitro*

The anti-tumour functionality of engineered CARs was assayed in a panel of Burkitt's lymphoma-derived cell lines, including three cell lines expressing Gb3 (Ramos, Raji, Daudi) and one cell line that was $Gb3^-$ (Namalwa) as assayed by flow cytometry using fluorescently labelled StxB (Fig. 2a). Importantly, all the cell lines expressed CD19, which is targeted by the anti-CD19-CAR T cells, here used as the positive control. Gb3 expression varied among the cell lines. Ramos cells expressed Gb3 the most (>99%), followed by Raji (88.3%) and Daudi (36.2%). By contrast, Gb3 was not detected in Namalwa cells. The amount of Gb3 on the cell surface also differed among the studied cell lines (Fig. 2a).

We next co-cultured lectin-CAR T cells with our selection of target cells (Ramos, Raji, Daudi and Namalwa) to assess the efficacy of tumour cell lysis. We implemented a cytotoxicity assay previously described [55] and adjusted the effector to target (E:T) ratio 5:1. We included three controls: activated but untransduced T cells, T cells that were activated and transduced with an empty vector (mock), and T cells that were activated and transduced with an anti-CD19-CAR. Shiga-CAR T cells performed best against all Gb3-expressing tumour cells. In particular, Ramos cells, which presented the highest Gb3 expression, were most efficiently eliminated, followed by Daudi and Raji cells (Fig. 2b-c and Fig. S2). After 48 h, the Shiga-CAR T cells achieved a specific killing (69.6%) of Ramos cells similar to anti-CD19-CAR T cells (90.3%), which served as a reference control in this and further experiments. Moreover, Shiga-CAR T cells achieved efficient killing of $Gb3^+$ Daudi cells since 36% of Daudi cells were $Gb3^+$, and on average, 40.6% of cells were killed in 48 h (Fig. 2b).

On the other hand, Raji cells seemed to be partially resistant to being targeted with Shiga-CAR T cells despite expressing high levels of Gb3 (99.8%) among the cells studied. Interestingly, Mitsuba-CAR T cells presented killing against Raji cells (26%, Fig. 2c), while the cytotoxicity against Ramos and Daudi was very low (<7.7%). LecA-CAR T cells displayed poor or no activity against this panel of cell lines. Importantly, none of the lectin-CAR T cells presented activity against the $Gb3^-$ Namalwa cells, demonstrating the specificity of the lectin-CARs and the lack of off-target killing. Anti-CD19-CAR T cells showed up to 95% cytotoxicity to all the CD19-expressing cell lines after 48 h (Fig. 2b-c).

T cells must actively and specifically recognise foreign antigens to mount an effective immune response. The antigen-induced signal over tonic signal can be used to determine effective T cell stimulation. Thus, we next analysed lectin-CAR T cell activation upon co-culturing with $Gb3^+$ and $CD19^+$ Ramos cells in a 5:1 effector to target cells for 48 h. We then determined the expression of the T cell activation markers CD137 and CD25 in BFP^+CD3^+ lectin-CAR T cells by flow cytometric analysis. Both $CD8^+$ and $CD4^+$ Shiga-CAR T cells displayed a substantial and significant increase in CD25 expression after exposure to $Gb3^+$ Ramos cells (Fig. 3a-c). $CD8^+$ and $CD4^+$ LecA-CAR T cells slightly increased CD25 expression upon contact with $Gb3^+$ Ramos cells, while Mitsuba-CAR T cells failed to recognise or establish a sustained binding to target cells and maintained similar CD25 expression compared to mock cells. Anti-CD19-CAR T cells exhibited strong CD25 expression after CD19 stimulation (Fig. 3a-c).

In contrast to CD25, none of the lectin-CAR T cells upregulated CD137 upon contact with $Gb3^+$ Ramos cells (Fig. 3d-f). These results are in sharp contrast with the behaviour of the anti-CD19-CAR T cells, which strongly increased the expression of CD137 upon incubation with $CD19^+$ Ramos cells (Fig. 3d-f). Despite having identical signalling domains, these data suggest differences in signal strength and quality between the lectin-CARs and the anti-CD19 CAR. Differential behaviour could be explained mechanistically by differences in clustering geometry, ligand density, or both.

Improving activation and cytotoxicity of lectin-CAR T cells

To assess potential confounding effects imparted by the different proportions of primary T cells expressing each lectin-CAR, we sorted BFP^+ cells to obtain homogeneous transduced populations. Upon sorting, cells were maintained in culture for 48 h to recover. The sorted CAR T cells were then co-incubated with $Gb3^+$ Ramos and $Gb3^-$ Namalwa cells, as described earlier. After 48 h, Shiga-CAR T cells achieved 75% of specific killing against Ramos cells, similar to unsorted cells 69.6% (Fig. 2b and Fig. 4a). Surprisingly, enrichment of Mitsuba-CAR T cells and LecA-CAR T cells allowed a remarkable increase in anti-tumour activity compared to unsorted cells (7.7% vs 27.8% and 2.2% vs 55.%, respectively; Fig. 2b and Fig. 4a), demonstrating that these CAR constructs were indeed functional. Moreover, sorting of the lectin-CAR T cells did not alter their specificity since their cytotoxic activity towards Namalwa cells was very poor or absent. The cytotoxicity of sorted anti-CD19-CAR T cells against Ramos and Namalwa was slightly higher compared to unsorted cells (90.3% vs 98.3%; Fig. 2b and Fig. 4a). Taken together, sorted lectin-CAR T cells accurately recognised and killed $Gb3^+$ cells lacking undesired off-target effects. The Shiga-CAR T cells were the best in targeting Gb3-expressing cells among the lectin-CAR T cells

One of the hallmarks of activated T lymphocytes is the production of cytokines, which in turn activate efficient immune responses. In contrast to anti-CD19-CAR, lectin-CARs efficiently drove upregulation of CD25, but not of CD137 (Fig. 3). Therefore, it was essential to evaluate whether lectin-CARs induced the secretion of cytokines. We co-cultured BFP^+-sorted cells with Ramos or Namalwa cells for 48 h and collected the supernatants to analyse cytokine release by ELISA. We tested the secretion of IFN-γ and TNF-α in response to co-cultures with $Gb3^+$ Ramos cells and $Gb3^-$ Namalwa cells. Shiga-CAR T cells efficiently and specifically secreted IFN-γ to the supernatant upon incubation with Ramos leukaemia cells (340 $pgml^{-1}$, Fig. 4b) compared to incubation with $Gb3^-$ Namalwa cells (Fig. 4b). However, LecA-CAR and Mitsuba-CAR T cells did not secrete IFN-γ above the background levels when stimulated with $Gb3^+$ Ramos or $Gb3^-$ Namalwa cells (Fig. 4b). The anti-CD19-CAR T cells released IFN-γ to the same extent as Shiga-CAR T cells when incubated with Ramos

cells (390 $pgml^{-1}$, Fig. 4b). TNF-α secretion by lectin-CAR T cells that were co-incubated with $Gb3^+$ Ramos cells was lower, 78 $pgml^{-1}$ for the Shiga-CAR, 45 $pgml^{-1}$ for the LecA-CAR T cells and Mitsuba-CAR T cells failed to produce TNF-α (Fig. 4c). TNF-α secretion by Shiga-CAR T cells was specific to the recognition of Gb3 since it was absent upon incubation with $Gb3^-$ Namalwa leukaemia cells. Anti-CD19-CAR T cells released considerably higher amounts of TNF-α (217 $pgml^{-1}$) upon incubation with Ramos cells.

In summary, these data indicate that Shiga-CAR T cells specifically produced cytokines upon recognition of Gb3 on the surface of target leukaemic cells. While Shiga-CAR T cells secreted as much IFN-γ as anti-CD19-CAR T cells, they secreted less TNF-α, which could be indeed beneficial to reduce the risk of cytokine release syndrome, a well-described life-threatening secondary effect in patients treated with anti-CD19-CAR T cells [56, 57].

Specificity of lectin-CAR T cells

Shiga-CAR T cells displayed the best anti-tumour activity against high $Gb3^+$ expressing Ramos leukaemic cells. To formally demonstrate that the Shiga-CAR T cells specifically target Gb3, Ramos cells were treated with PPMP to inhibit the synthesis of glucosyl-ceramide based glycosphingolipids. PPMP is a ceramide analogue designed to inhibit the glycosyltransferase involved in the biosynthesis of glucosylceramides [58], primary reducing the expression of Gb3 [59]. Ramos cells were exposed to 1 μM and 2 μM of PPMP for 3 days. On the third day, the levels of Gb3 on the cell surface were assessed by staining the cells with fluorescently labelled StxB. Flow cytometric analysis showed that PPMP treatment efficiently reduced the levels of Gb3 on the cell surface of Ramos cells, similar to unstained cells (Fig. S3a). Cells treated with PPMP or vehicle (dimethyl sulfoxide, DMSO) were co-cultured with Shiga-CAR T cells and controls, mock and anti-CD19-CAR T cells. PPMP-treated Ramos cells were significantly less killed by Shiga-CAR T cells after 12 h (36%, 1 μM, and 26%, 2 μM) and 24 h (54% and 46%, respectively) compared to untreated or vehicle-treated Ramos cells (both >56% at 12 h and both >75% at 24 h, Fig. 5a and Fig. S3b). The reduction was dose-dependent with decreased cytotoxicity at higher concentrations of PPMP. The treatment with PPMP did not affect the viability of Ramos cells or the presence of CARs on the T cell surface (Fig. S3c-d). Moreover, the cytotoxic activity of controls, mock and anti-CD19-CAR T cells, remained unaffected. Taken together, these data argue strongly for a specific cytotoxic effect following Gb3-dependent activation of lectin-CARs.

Gb3 recognition in cell-sized giant unilamellar vesicles by Shiga-CAR T cells

Next, we applied a simplified and controlled membrane system to demonstrate that the presence of Gb3 is sufficient for recognition by Shiga-CAR T cells. Giant unilamellar vesicles (GUVs) are synthetic cell-sized spherical lipid bilayers resembling the size of human cells that can be glyco-decorated with diverse glycans [60, 61]. They have been explored to rebuild and, therefore, to better understand cellular processes, e.g., adhesion [62] and endocytosis [60, 63]. We produced GUVs containing 10 mol% Gb3 within the chosen lipid mixture (DOPC, cholesterol, Atto 647N-DOPE and Gb3; 59.7: 30: 0.3: 10 mol%, respectively) by electroformation [50]. On the day of the experiment, sorted Shiga-CAR T cells or mock T cells were stained with the CellTrace ^{TM} CFSE reagent for visualisation by confocal microscopy. The GUVs were visible in far-red. GUVs and T cells were co-incubated and monitored for 30 min at 37°C. We acquired distinct areas using a live cell imaging setting by confocal microscopy. The Shiga-CAR T cells and mock T cells continuously approached GUVs and surrounded them. The interactions between Shiga-CAR T cells and GUVs were more likely than

with mock T cells (Online Resource-1-2). Over time, more and more cells enriched the areas around the GUVs as trying to build contacts. In some cases, the Gb3-containing GUVs were deformed exclusively during the interactions with Shiga-CAR T cells. Such events were not observed upon incubation with mock cells (Fig. 5b). Inward bending of $Gb3^+$ GUVs probably indicate tight interactions of Shiga-CAR T cells with Gb3-functionalised vesicles, related to membrane invaginations induced by StxB [64, 65] or LecA in $Gb3^+$ GUVs and HEK cells [43, 66]. More recently, a molecular dynamics simulation also proposed the induction of negative membrane curvature triggered by StxB and LecA after binding to and clustering of Gb3 [68].

To quantify these interactions, we analysed the contact between GUVs and T cells using the Ilastik software [51]. For this purpose, a protocol for machine learning was developed, and time series were analysed after image segmentation. The contact between GUVs and cells was estimated using percent of contact. The quantification of pixels in green (cells), red (GUVs), and co-localised were considered to calculate the percent of contact, which was determined for each monitored area and time point. The analysis revealed cell interactions in both conditions, but the percent of contact was higher for the Shiga-CAR T cells than for the mock T cells (Fig. 5c). These results suggest that Gb3 drives the interactions with the Shiga-CAR T cells. This interaction might occur independently of any additional protein on the surface of target cells, as we used a synthetic system lacking additional proteins or active cellular machinery.

As briefly mentioned above, the interactions between the homopentameric StxB and Gb3 in synthetic membrane systems and living cells is well documented in the literature [64, 69]. Considering that only a single StxB monomer was part of the CAR construct, it was somewhat surprising to observe that StxB monomers in the framework of CARs might facilitate these interactions. Additionally, Shiga-CARs showed dimers and trimers in primary T cells (Fig. 1), which might increase the avidity for Gb3 on the GUV and host cell membrane. Taken together, we successfully demonstrated that Gb3 and the GUV environment were sufficient to drive the interactions with the carbohydrate-binding domain of the Shiga-CAR, strongly supporting the selectivity of our approach.

Lectin-CAR T cells efficiently target solid tumour cell lines

One of the major obstacles for using CAR T cell technology against solid tumours is the lack of tumour-specific antigens [70, 71]. Since Gb3 is overexpressed in colorectal carcinoma [32], breast [33], ovary and pancreatic cancer [34], as well as gliomas [35], we decided to test the anti-tumour activity of the lectin-CARs against cell lines derived from colon and breast cancer. First, we checked the expression of Gb3 in a panel of cells by staining them with fluorescently labelled StxB (Fig. 6a). Flow cytometry analysis revealed that colorectal cancer cell lines HT-29 and HCT-166 expressed Gb3 (> 95% positive cells). MDA-MB-231 cells heterogeneously expressed Gb3, with 83% positive cells overall. In contrast, Gb3 was not detected in LS-174 colorectal cancer cells and JIMT1 breast cancer cell lines.

Next, we performed cytotoxic assays using our complete panel of primary lectin-CAR T cells. Similarly to the results obtained for leukaemia cells, Shiga-CAR was the best targeting Gb3 (Fig. 6b-c and Fig. S4). Shiga-CAR T cells showed the highest anti-tumour activity against HT-29 (74%) and HCT-166 (90%) colorectal cancer cells and MDA-MB-231 triple-negative breast tumour cells (60%). The possibility of targeting triple-negative breast cancer cells with lectin-CAR T cells is remarkable. Triple-negative breast cancer is the most aggressive and lethal breast cancer subtype, for which no targeted treatment options are currently available [72]. Mitsuba-CAR T cells displayed cytotoxic activities varying

between 40% and 60% among the cell lines expressing Gb3, namely HT-29, HCT-166 and MDA-MB-231. Meanwhile, the cytotoxicity exhibited by LecA-CAR T cells was the lowest (10-24%) compared to other lectin-CARs and showed a high intrinsic variation among individual donors. Taken together, lectin-CARs efficiently targeted $Gb3^+$ colorectal and breast cancer cells while lacking cytotoxicity against $Gb3^-$ tumour cells, supporting once more the specificity of Gb3 recognition. The recognition of cell lines derived from solid tumours by lectin-CAR T cells appears to be even more efficient than the recognition of leukaemic cells.

Next, we sorted BFP^+ CAR T cells and investigated whether the killing activity could be enhanced when working with pure CAR T cell populations as previously observed (Fig. 4). Using pure populations, Mitsuba-CAR (92% and 84%) and LecA-CAR T cells (85% and 79%) achieved similar killing activity as Shiga-CAR T cells (99.8% and 83%) when co-incubated with HT-29 and HCT-116 tumour cells (Fig. 6d). In this way, anti-tumour activity was also enhanced, and the percentage of killed cells increased at the endpoint of the experiment. The anti-tumour activity of the LecA-CAR and Mitsuba-CAR in solid tumours appears to be vastly improved. The performance of lectin-CARs against cell lines derived from colorectal cancer and breast cancer is promising, considering the previous lack of cancer-specific targets.

Lectin-CARs recognise a wide variety of Gb3 isoforms

Glycosphingolipids represent approximately 3% of the extracellular leaflet of the plasma membrane [73]. To better understand the influence of Gb3 abundance and diversity on the recognition by lectin-CAR T cells, we characterised the amount of Gb3 isoforms, which can vary in fatty acyl chain length, degree of saturation and hydroxylation, in several of the target cells used in this study (HT-29, Ramos, MDA-MB-231, Namalwa and LS-174). Cells were lysed in a mixture of methanol and water 1:1, followed by chloroform purification, which allowed lipid isolation for later targeted liquid chromatography and mass spectrometry. The normalised intensities indicate the total abundance of Gb3 (Fig. 7a). HT-29 cells (0.028) exhibited the highest total amount of Gb3, followed by Ramos (0.018) and MDA-MB-231 (0.015) cells. Namalwa (0.002) had little Gb3 content, and Gb3 was not detected in LS-174 cells (Fig. 7a), confirming our flow cytometric data (Fig. 2a and Fig. 6a). We next performed a Pearson correlation between the total Gb3 abundance detected by MS analysis in each cell line and the cytotoxicity of the lectin-CAR T cells. We aimed to understand whether the abundance of Gb3 influences the efficacy of the lectin-CAR T cells in lysing cells. The analysis revealed a solid Gb3 dependency for the Shiga-CAR T cell-induced cytotoxicity ($r_{Shiga\text{-}CAR}$=0.9742) and a moderate dependency for LecA-CAR T cells ($r_{LecA\text{-}CAR}$ =0.7274) and Mitsuba-CAR T cells ($r_{Mitsuba\text{-}CAR}$ =0.6197). In general, the higher is the abundance of Gb3 on the target cells, the higher is the cytotoxicity (Fig. S6). However, a deeper analysis of the dominantly present Gb3 species revealed that the studied model cells lines contain many Gb3 isoforms. In HT-29 colorectal cancer cells, the isoform C16:0-OH and C16:0 each made up 25% of the Gb3 species present. The saturated species C24:0 represented 19%, and its hydroxylated isoform C24:0-OH 13%. Additionally, 6% of C22:0 and small traces of C18:1; C18:0, C20:0, C24:1-OH, C22:0-OH and C24:1 were detected (Fig. 7b). Interestingly, hydroxylated Gb3 isoforms, which have been little reported so far, were present in HT-29 cells. These isoforms seemed to be highly relevant for the scission of StxB-induced tubular membrane invaginations [74]. In Ramos leukaemic cells, the non-saturated isoform C24:1 constituted 39% of the total Gb3. The saturated C16:0 and 24:0 isoforms represented around 20% each, the C22:0 isoform only 9% and the C18:0 isoform around 5% of the total Gb3 amount. Small traces of other isoforms included C16:0-OH, C18:1, C20:0, C24:1-OH, C22:0-OH and C24:0-OH (Fig. 7c). In MDA-MB-231 triple-negative breast cancer cells, 42% of the

isoforms were designated to C24:0 and 26% to its unsaturated form C24:1. About 22% were matched to the C16:0 and only 7% to the C22:0 Gb3 isoform. The remaining C16:0-OH, C18:1, C20:0, C24:1-OH, C22:0-OH and C24:0-OH were detected only in trace amounts (Fig. 7d). In Namalwa and LS-174 cells, hardly any Gb3 isoform was detected (Fig. S5). These results are alternatively depicted as a heat map in Fig. S5, clearly showing that each model cell line has a unique profile of Gb3 isoforms.

It has been reported that the length and degree of saturation of different Gb3 isoforms affect the binding of StxB and LecA in their native conformation [32, 47, 69, 75]. However, the influence of the structure of each Gb3 isoform on lectin-CAR T cell binding is entirely unknown. Thus, we performed a correlation analysis between the abundance of each Gb3 isoform and the cytotoxicity of different lectin-CAR T cells. We aimed to identify Gb3 isoforms that might be preferentially recognised by a given lectin-CAR independently of the cell line. The correlation coefficients are represented as a heat map (Fig. 7e). According to this, the Shiga-CAR T cells seemed to prefer the C18:1, C16:0, and C22:0 isoforms. Hydroxylation of these isoforms reduced recognition by nearly 50%. In contrast, hydroxylation of the C24:1 isoform increased 3 times the recognition by Shiga-CAR T cells. LecA-CAR T cells correlation values suggest a better recognition of the C24:0, C16:0 and the C18:1. Again, the hydroxylated isoforms were less preferred, reducing the specific killing to half. The Mitsuba-CAR T cells equally favoured C18:1, C22:0 and C24:0, and recognition of hydroxylated forms was also reduced. Taken together, we observed that the C18:1, C24:0, C16:0, C22:0 have the highest correlation coefficients, and they may be the best recognised isoforms. Strikingly, the C18:1 is present in very low amounts in the three model cell lines. It is remarkable that hydroxylation of these isoforms significantly reduced recognition by all lectin-CAR T cells. In summary, the correlation analysis indicates that the specific recognition of Gb3 by lectin-CARs is robust as they could target a wide variety of Gb3 isoforms present in the target cells.

Discussion

One of the biggest challenges in oncology is to find novel molecular targets and strategies to selectively target and eliminate cancer cells. Therapies targeting tumour-associated carbohydrate antigens in combination with the anti-cancer efficacy of CAR T cells may unlock attractive and powerful treatment options hitherto underutilised. In light of this, we explored a strategy to target the glycosphingolipid Gb3 using novel lectin-based CARs. Our study demonstrates that lectin-CAR T cells, which specifically recognise Gb3, induced the killing of several cancer types. Our approach serves as proof of concept for developing specific lectin-CARs targeting other tumour associated carbohydrate antigens.

We created a collection of lectin-CARs that employed distinct Gb3-binding lectins as binding domains, such as the lectin LecA from *Pseudomonas aeruginosa*, the B-subunit of Shiga toxin mainly produced by *Shigella dysenteriae* and *Escherichia coli* strains, and the computationally designed lectin Mitsuba [42, 44]. The successful use of STxB for *in vivo* targeting of $Gb3^+$ xenografts [76, 77] and the study of LecA as a drug delivery system [20, 78] in $Gb3^+$ cells inspired the design of the lectin-CARs.

Lectin-CARs, in particular the Shiga-CAR, exhibited cytotoxicity against the Burkitt's lymphoma-derived cell lines (Ramos (75.5%), Raji (26%) and Daudi (40%)), which, like other B-lymphoma cell lines, also express and accumulate Gb3 at their cell surfaces [31, 39]. Interestingly, the Shiga-CAR T cells showed that they could reach a cytotoxic activity comparable to anti-CD19-CAR T cells (>75%). CAR-T cell therapy has achieved good objective responses in diffuse large B cell

lymphoma, although their efficacy in adult Burkitt's lymphoma remains limited to a few reports with variable response rates. In these case reports, anti-CD19-CAR T cells have been used to target malignant and healthy B cells, often leaving the patients with long-term B-cell aplasia and hypogammaglobulinemia. Hypogammaglobulinemia, a pathological decrease in antibody production, renders these patients susceptible to potentially life-threatening infections [79, 80]. Studies have demonstrated that anti-CD19-CAR T cells could persist for years in patients who require expensive and recurrent treatments to reconstitute their immunoglobulin levels and keep protection against opportunistic infections [81, 82]. Lectin-CARs might thus represent an alternative and a potential treatment for haematological malignancies to overcome limitations such as life threatening-associated toxicities, poor responses to anti-CD19-CAR T cells, antigen escape and resistance in B cell malignancies.

Besides to B cell malignancies, the lectin-CAR T cells displayed anti-tumour activity towards the colorectal cancer cell lines HT-29 and HTC-116. A killing efficacy of up to 99.8% was achieved by Shiga-CAR and 92% by Mitsuba-CAR, respectively. Colorectal cancer is the cancer type with the highest number of patients analysed for Gb3 expression. These studies showed an increase in Gb3 expression compared to normal or benign colonic tissue [32, 34, 41]. Moreover, it has been reported that colon cancer metastasis is Gb3-dependent, and therefore, targeting Gb3 can inhibit the progression of these tumours.

We have also investigated the cytotoxicity of lectin-CAR T cells towards the MDA-MB-231 triple-negative breast cancer cells. Triple-negative breast cancer is the most aggressive and lethal breast cancer subtype, for which, to date, we are lacking successful targeted treatments [72, 83]. Lectin-CAR T cells, in particular, the LecA-CAR, effectively recognised and lysed MDA-MB-231 cells with a killing efficacy of 59.7%. Most of the primary breast cancer tumours and breast cancer cell lines (70-80%) overexpress Gb3 compared to normal tissue [31, 37]. Notably, the lectin-CAR T cells were specific for Gb3 and did not exhibit off-target cytotoxicity as demonstrated using $Gb3^{-}$ tumour cells such as LS-174 and JIMT1.

The notable performance of the lectin-CAR T cells against cells derived from solid tumours and haematological malignancies promises a comprehensive application. Gb3 is present in many additional tumour types such as lung, testicular, and ovarian cancer [39, 84]. In addition to directly targeting the tumour cells, lectin CAR-T cells might provide a benefit by targeting the tumour vasculature because Gb3 has been predominantly found in tumour blood vessels [85]. In fact, a neuroblastoma study demonstrated that Gb3 targeting prevented tumour angiogenesis [86]. Gb3 has also been associated with multi-drug resistance in lung and breast cancer and chronic myeloid leukaemias [38, 85, 87]. Gb3 is co-expressed and interplays with efflux transporters such as ATP-binding cassette, resulting in the active efflux of several chemotherapeutic agents. These anti-cancer agents stimulate Gb3 and enhance the expression of proteins that contribute to multi-drug resistance, resulting in a severely reduced effectivity of chemotherapeutic drugs [88–90]. Lectin-CAR T cells could be used as second-line therapy in the treatment of drug-resistant cancers.

There are many scenarios in which the Gb3-binding lectin-CARs could be applied, considering that the number of effective treatments for solid tumours is still very limited. The feasibility of the application of lectin-CAR T cells against cancer depends on at least two Gb3-related factors: the abundance of Gb3 on the cell surface of normal and cancer cells and the heterogenicity in the structure of Gb3, which defines the degree of recognition by different lectin-CAR T

cells. Firstly, our MS analysis revealed that Gb3 abundance varied between model tumour cell lines; Gb3 is at least 30% more abundant in HT-29 cells than in Ramos and MDA-MB-231 cells. In comparison, Gb3 was barely detected in Namalwa and not detected in the LS-174 cells. Our analysis exposed a strong-to-moderate dependency between Gb3 abundance and specific killing by the lectin-CAR T cells, especially when pure populations of lectin-CAR T cells were employed. Thus, Gb3 abundance determines lectin binding, as previously reported [91], thereby the recognition and cytotoxic activity of the lectin-CAR T cells. Secondly, the natural heterogenicity of Gb3 regarding chain length, degree of saturation and hydroxylation of its fatty acyl chain impact lectin binding [29, 69, 91–93]. To identify whether the structural variability of Gb3 also influences the ability of the lectin-CAR T cells to target $Gb3^+$ cancer cell lines, we performed an MS screening to characterise the Gb3 isoforms in each of the selected cells lines. We then completed a correlation analysis between Gb3 isoforms and the cytotoxicity of lectin-CAR T cells. The MS analysis brought to light the heterogeneity of Gb3 and revealed distinct Gb3 isoform profiles for the different model cell lines. In Ramos and MDA-MB-231 cells, the most abundant Gb3 isoforms were Gb3(d18:1/C16:0), Gb3(d18:1/C24:0) and Gb3(d18:1/C24:1), in line with a previous report [94]. In contrast, the most common isoforms present in the HT-29 cell line were Gb3(d18:1/C16:0), Gb3(d18:1/C24:0) and, unexpectedly, Gb3(d18:1/C16:0-OH). Additional species with little presence, e.g. Gb3(d18:1/C22:0) and Gb3(d18:1/C18:1), were also detected and considered in further analysis. These species, although marginally expressed, may play a critical role in lectin-CAR recognition. On the one hand, the highest correlation coefficient with the cytotoxicity of Shiga-CAR T cells was obtained for Gb3(d18:1/C18:1), Gb3(d18:1/C16:0), and Gb3(d18:1/C22:0), which probably are the preferred Gb3 isoforms. Following these results, it has been reported that C18:1 and C22:0 were the most effective fatty acyl chains for StxB binding, in particular at lower receptor concentrations [91, 92]. According to the calculated correlation coefficients, it seems that the hydroxylated Gb3 species, which were not yet very often described, also play a role in the binding and activation of Shiga-CAR T cells. In line with Schütte et al. and Römer et al., who have shown that hydroxylated species are important for the scission of STxB-induced membrane tubules [74, 95]. On the other hand, the highest correlation coefficient for the LecA-CAR T cells was registered for the Gb3(d18:1/C24:0) isoform. This result is consistent with a recent report, suggesting that Gb3(d18:1/C24:0) is indeed the preferred Gb3 isoform of LecA [47]. Taken together, the Shiga-CAR and LecA-CAR T cells well reflected the Gb3 preferences previously described for StxB and LecA in their native forms. In contrast, the preferences of the engineered Mitsuba lectin for the different Gb3 isoforms have not been studied yet. The highest correlation coefficients for the Mitsuba-CAR T cells were found for Gb3(d18:1/C18:1), Gb3(d18:1/C24:0) and Gb3(d18:1/C22:0). These data may thus give a hint to the preferred species of this lectin for future studies. Interestingly, each of the lectin-CAR T cells studied herein recognised several Gb3 species. This ability could be an advantage since the heterogeneous expression of an antigen is a major limitation for effective tumour targeting by CAR T cells [96].

In our study, the recognition of the Gb3 isoforms might also be influenced by the efficiency of the lectin-CAR constructs to be expressed on the T cell surface. The LecA-CAR was detected at high levels on the cell surface of primary T cells, while the Shiga-CAR and Mitsuba-CAR were detected at lower levels. The low detection could be due to different reasons, e.g., an alternative protein folding preventing the binding of the anti-FLAG antibody; it might also be the consequence of CAR degradation or less efficient export to the plasma membrane due to the lectin domain of bacterial origin. Despite little being known about the expression of bacterial proteins in mammalian cells, it has been reported

that some degree of glycosylation, specifically N-glycosylation, is required for the correct folding of bacterial proteins destined for the extracellular space [97]. We must also consider that human glycosylation patterns that can modify the lectin domains. Additionally, the cryptic signals present in bacterial gene sequences might negatively impact intracellular trafficking pathways of mammalian cells [98]. Altogether, this might explain the lower detection level of Gb3-binding lectin-CARs on the cell surface. A similar phenomenon has been observed for the expression of cholera toxin the B-subunit and the tetanic toxin C in mammalian cells [99, 100]. Despite that, the expression levels were enough to perform efficient CAR T cell recognition activation and elimination of the target cells.

The use of lectins as a binding motif in CAR T cells can be complementary or alternative to other therapeutic approaches such as antibodies targeting TACAs. On the one hand, generating antibodies with a high affinity for TACAs can be challenging due to the low immunogenicity and immune tolerance of these structures. On the other hand, lectins naturally and specifically recognise TACAs [15, 101, 102]. The engineering of lectins opens up a world of possibilities with lectins of tailored valency and affinity [103], different number of subunits [104] or reduced immunogenicity, e.g. Mitsuba [45], that would allow broader use of these carbohydrate-binding proteins.

Conclusions and outlook

In summary, we demonstrate that Gb3-binding lectin-CAR T cells recognise multiple Gb3 isoforms present in different cancers types. The cytotoxicity of Shiga-CAR T cells against several Burkitt's lymphoma and solid tumour cells was the most prominent among the panel of studied lectin-CARs. However, LecA-CAR and Mitsuba-CAR T cells also showed promising activity in specific cases, which may be due to a delimited recognition of Gb3 species.

In vivo studies will be conducted in the near future to investigate the behaviour of Gb3-binding lectin-CAR T cells in model organisms. They would also help to clarify open questions regarding which specific lectin to best use, and which Gb3 isoform is safest and most effective for targeting. Although the clinical translation of these findings remains to be done, we have herewith demonstrated the feasibility of targeting cancer cells by using novel and innovative lectin-CAR constructs.

Supplementary Information

The online version contains supplementary material available.

Acknowledgements

We thank the Lighthouse Core Facility staff of the Medical Center - University of Freiburg for their help with their cell sorting resources and excellent support. In addition, we would like to express our gratitude to the Life Imaging Center (LIC) of the University of Freiburg for support. We also wish to thank Dr. Pavel Salavei of the CIBSS Signaling Factory, University of Freiburg, Germany, for his support in flow cytometry. Ana Valeria Meléndez and Oliver S. Thomas are grateful for support from the Spemann Graduate School of Biology and Medicine (SGBM).

Author's contributions

Conception and design of the research: Ana Valeria Meléndez, Susana Minguet and Winfried Römer. Funding acquisition: Wilfried Weber, Bernd Kammerer, Susana Minguet and Winfried Römer. Investigation: Ana Valeria

Meléndez, Rubí M-H Velasco Cárdenas, Simon Lagies, Oliver S. Thomas and Lina Siukstaite. Methodology: Rubí M-H Velasco Cárdenas, Simon Lagies, Oliver S. Thomas and Lina Siukstaite. Supervision: Wilfried Weber, Bernd Kammerer, Susana Minguet and Winfried Römer. Writing-original draft: Ana Valeria Meléndez. Writing –review & editing: Rubí M-H Velasco Cárdenas, Simon Lagies, Oliver S. Thomas, Lina Siukstaite. Winfried Römer and Susana Minguet. All authors approved the final version of the manuscript.

Funding

Open Access funding enabled and organised by Projekt DEAL. This project was supported by the Deutsche Forschungsgemeinschaft (DFG, German Research Foundation) under Germany's Excellence Strategy (GSC-4, EXC-294 and EXC-2189) and the German Research Foundation grant Major Research Instrumentation (project number: 438033605), by the Ministry for Science, Research and Arts of the State of Baden-Württemberg (Az: 33-7532.20; and partial funding of SGBM PhD thesis) and by the Freiburg Institute for Advanced Studies (FRIAS). Moreover, this research was funded by the European Union's Horizon 2020 Research and Innovation Programme under the Marie Skłodowska-Curie grant agreement synBIOcarb (No. 814029). The lab of SM is supported by the German Research Foundation with the projects SFB1160 (B01), SFB1479 (Project ID: 441891347 - P15) and FOR2799 (MI1942/3-1).

Data availability

The datasets generated and/or analysed during the current study are available from the corresponding authors on reasonable request.

Conflict of interest

No potential conflict of interest relevant to this article was reported.

Ethics approval

Buffy coats used as blood sources were purchased from the blood bank of the University Medical Centre Freiburg (approval of the University Freiburg Ethics Committee: 147/15).

Consent to participate

Not applicable.

References

1. Kochenderfer, J. N., Wilson, W. H., Janik, J. E., Dudley, M. E., Stetler-Stevenson, M., Feldman, S. A., … Rosenberg, S. A. (2010). Eradication of B-lineage cells and regression of lymphoma in a patient treated with autologous T cells genetically engineered to recognise CD19. *Blood*, *116*(20). https://doi.org/10.1182/blood-2010-04-281931

2. Batlevi, C. L., Matsuki, E., Brentjens, R. J., & Younes, A. (2016). Novel immunotherapies in lymphoid malignancies. *Nature Reviews Clinical Oncology*. https://doi.org/10.1038/nrclinonc.2015.187

3. Maher, J., Brentjens, R. J., Gunset, G., Rivière, I., & Sadelain, M. (2002). Human T-lymphocyte cytotoxicity and proliferation directed by a single chimeric TCRζ/CD28 receptor. *Nature Biotechnology*, *20*(1). https://doi.org/10.1038/nbt0102-70

4. Majzner, R. G., & Mackall, C. L. (2018). Tumor Antigen Escape from CAR T-cell Therapy Mini review ABstrAct. *CANCER DISCOVERY*.

5. Sterner, R. C., & Sterner, R. M. (2021). CAR-T cell therapy: current limitations and potential strategies. *Blood Cancer Journal*. https://doi.org/10.1038/s41408-021-00459-7

6. Varki, A. (2017). Biological roles of glycans. *Glycobiology*, *27*(1). https://doi.org/10.1093/glycob/cww086

7. Kobata, A., & Amano, J. (2005). Altered glycosylation of proteins produced by malignant cells, and application for the diagnosis and immunotherapy of tumours. *Immunology and Cell Biology*, *83*(4). https://doi.org/10.1111/j.1440-1711.2005.01351.x

8. Stowell, S. R., Ju, T., & Cummings, R. D. (2015). Protein Glycosylation in Cancer. *Annual Review of Pathology: Mechanisms of Disease*. https://doi.org/10.1146/annurev-pathol-012414-040438

9. Varki, A., Esko, J. D., & Colley, K. J. (2009). *Cellular Organization of Glycosylation*. *Essentials of Glycobiology*. https://doi.org/NBK1926 [bookaccession]

10. Dingjan, T., Spendlove, I., Durrant, L. G., Scott, A. M., Yuriev, E., & Ramsland, P. A. (2015). Structural biology of antibody recognition of carbohydrate epitopes and potential uses for targeted cancer immunotherapies. *Molecular Immunology*. https://doi.org/10.1016/j.molimm.2015.02.028

11. Christiansen, M. N., Chik, J., Lee, L., Anugraham, M., Abrahams, J. L., & Packer, N. H. (2014). Cell surface protein glycosylation in cancer. *Proteomics*. https://doi.org/10.1002/pmic.201300387

12. Ghazarian, H., Idoni, B., & Oppenheimer, S. B. (2011). A glycobiology review: Carbohydrates, lectins and implications in cancer therapeutics. *Acta Histochemica*. https://doi.org/10.1016/j.acthis.2010.02.004

13. Feizi, T. (1985). Carbohydrate antigens in human cancer. *Cancer Surveys*.

14. Ozkaynak, M. F., Gilman, A. L., London, W. B., Naranjo, A., Diccianni, M. B., Tenney, S. C., … Yu, A. L. (2018). A comprehensive safety trial of chimeric antibody 14.18 with GM-CSF, IL-2, and isotretinoin in high-risk neuroblastoma patients following myeloablative therapy: Children's oncology group study ANBL0931. *Frontiers in Immunology*, *9*(JUN). https://doi.org/10.3389/fimmu.2018.01355

15. Heimburg-Molinaro, J., Lum, M., Vijay, G., Jain, M., Almogren, A., & Rittenhouse-Olson, K. (2011). Cancer vaccines and carbohydrate epitopes. *Vaccine*. https://doi.org/10.1016/j.vaccine.2011.09.009

16. Bialecki, E. S., & Di Bisceglie, A. M. (2005). Diagnosis of hepatocellular carcinoma. *HPB*. https://doi.org/10.1080/13651820410024049

17. Pervin, M., Koyama, Y., Isemura, M., & Nakamura, Y. (2015). Plant Lectins in Therapeutic and Diagnostic Cancer Research. *International Journal of Plant Biology & Research*, *3*(2).

18. Lyu, S. Y., Kwon, Y. J., Joo, H. J., & Park, W. B. (2004). Preparation of alginate/chitosan microcapsules and enteric coated granules of mistletoe lectin. *Archives of Pharmacal Research*, *27*(1). https://doi.org/10.1007/BF02980057

19. S. Coulibaly, F., & C. Youan, B.-B. (2017). Current status of lectin-based cancer diagnosis and therapy. *AIMS Molecular Science*, *4*(1), 1–27. https://doi.org/10.3934/molsci.2017.1.1

20. Müller, S. K., Wilhelm, I., Schubert, T., Zittlau, K., Imberty, A., Madl, J., … Römer, W. (2017). Gb3-binding lectins as potential carriers for transcellular drug delivery. *Expert Opinion on Drug Delivery*, *14*(2). https://doi.org/10.1080/17425247.2017.1266327

21. Okuda, T. (2021). Application of the antibody-inducing activity of glycosphingolipids to human diseases. *International Journal of Molecular Sciences*. https://doi.org/10.3390/ijms22073776

22. Hakomori, S. I., & Murakami, W. T. (1968). Glycolipids of hamster fibroblasts and derived malignant-transformed cell lines. *Proceedings of the National Academy of Sciences of the United States of America*, *59*(1). https://doi.org/10.1073/pnas.59.1.254

23. Hakomori, S. I. (1996). Tumor malignancy defined by aberrant glycosylation and sphingo(glyco)lipid metabolism.

Cancer Research.

24. Hakomori, S. (2003). Structure, organisation, and function of glycosphingolipids in membrane. *Current Opinion in Hematology*. https://doi.org/10.1097/00062752-200301000-00004

25. Ito, M., Suzuki, E., Naiki, M., Sendo, F., & Arai, S. (1984). Carbohydrates as antigenic determinants of tumor-associated antigens recognised by monoclonal anti-tumor antibodies produced in a syngeneic system. *International Journal of Cancer*, *34*(5). https://doi.org/10.1002/ijc.2910340517

26. Hakomori, S. (1981). Glycosphingolipids in cellular interaction, differentiation, and oncogenesis. *Annual review of biochemistry*. https://doi.org/10.1146/annurev.bi.50.070181.003505

27. Kannagi, R., Fukuda, M. N., & Hakomori, S. (1982). A new glycolipid antigen isolated from human erythrocyte membranes reacting with antibodies directed to globo-N-tetraosylceramide (globoside). *Journal of Biological Chemistry*, *257*(8), 4438–4442. https://doi.org/10.1016/s0021-9258(18)34741-0

28. Schnaar, R. L. T., & Kinoshita, T. (2017). Chapter 11 Glycosphingolipids. *Essentials of glycobiology 3rd Edition*.

29. Pellizzari, A., Pang, H., & Lingwood, C. A. (1992). Binding of Verocytotoxin 1 to Its Receptor Is Influenced by Differences in Receptor Fatty Acid Content. *Biochemistry*, *31*(5). https://doi.org/10.1021/bi00120a011

30. Merrill, A. H. (2011). Sphingolipid and glycosphingolipid metabolic pathways in the era of sphingolipidomics. *Chemical Reviews*. https://doi.org/10.1021/cr2002917

31. LaCasse, E. C., Saleh, M. T., Patterson, B., Minden, M. D., & Gariépy, J. (1996). Shiga-like toxin purges human lymphoma from bone marrow of severe combined immunodeficient mice. *Blood*, *88*(5). https://doi.org/10.1182/blood.v88.5.1561.bloodjournal8851561

32. Falguières, T., Maak, M., Von Weyhern, C., Sarr, M., Sastre, X., Poupon, M. F., … Janssen, K. P. (2008). Human colorectal tumors and metastases express Gb3 and can be targeted by an intestinal pathogen-based delivery tool. *Molecular Cancer Therapeutics*, *7*(8). https://doi.org/10.1158/1535-7163.MCT-08-0430

33. LaCasse, E. C., Bray, M. R., Patterson, B., Lim, W. M., Perampalam, S., Radvanyi, L. G., … Gariépy, J. (1999). Shiga-like toxin-1 receptor on human breast cancer, lymphoma, and myeloma and absence from CD34+ hematopoietic stem cells: Implications for ex vivo tumor purging and autologous stem cell transplantation. *Blood*, *94*(8). https://doi.org/10.1182/blood.V94.8.2901.420k36_2901_2910

34. Distler, U., Souady, J., Hülsewig, M., Drmić-Hofman, I., Haier, J., Friedrich, A. W., … Müthing, J. (2009). Shiga toxin receptor Gb3Cer/CD77: Tumor-association and promising therapeutic target in pancreas and colon cancer. *PLoS ONE*, *4*(8). https://doi.org/10.1371/journal.pone.0006813

35. Johansson, D., Johansson, A., Grankvist, K., Andersson, U., Henriksson, R., Bergström, P., … Behnam-Motlagh, P. (2006). Verotoxin-1 induction of apoptosis in Gb3-expressing human glioma cell lines. *Cancer Biology and Therapy*, *5*(9). https://doi.org/10.4161/cbt.5.9.3173

36. Cooling, L. L. W., Zhang, D. S., Naides, S. J., & Koerner, T. A. W. (2003). Glycosphingolipid expression in acute non-lymphocytic leukemia: Common expression of shiga toxin and parvovirus B19 receptors on early myeloblasts. *Blood*, *101*(2). https://doi.org/10.1182/blood-2002-03-0718

37. Stimmer, L., Dehay, S., Nemati, F., Massonnet, G., Richon, S., Decaudin, D., … Johannes, L. (2014). Human breast cancer and lymph node metastases express Gb3 and can be targeted by STxB-vectorized chemotherapeutic compounds. *BMC Cancer*, *14*(1). https://doi.org/10.1186/1471-2407-14-916

38. Gupta, V., Bhinge, K. N., Hosain, S. B., Xiong, K., Gu, X., Shi, R., … Liu, Y. Y. (2012). Ceramide glycosylation by glucosylceramide synthase selectively maintains the properties of breast cancer stem cells. *Journal of Biological Chemistry*, *287*(44). https://doi.org/10.1074/jbc.M112.396390

39. Engedal, N., Skotland, T., Torgersen, M. L., & Sandvig, K. (2011). Shiga toxin and its use in targeted cancer therapy and imaging. *Microbial Biotechnology*. https://doi.org/10.1111/j.1751-7915.2010.00180.x

40. Skotland, T., Kavaliauskiene, S., & Sandvig, K. (2020). The role of lipid species in membranes and cancer-related changes. *Cancer and Metastasis Reviews*. https://doi.org/10.1007/s10555-020-09872-z

41. Kovbasnjuk, O., Mourtazina, R., Baibakov, B., Wang, T., Elowsky, C., Choti, M. A., … Donowitz, M. (2005). *The glycosphingolipid globotriaosylceramide in the metastatic transformation of colon cancer*. Retrieved from www.pnas.orgcgidoi10.1073pnas.0506474102

42. Siukstaite, L., Imberty, A., & Römer, W. (2021). Structural Diversities of Lectins Binding to the Glycosphingolipid Gb3. *Frontiers in Molecular Biosciences*. https://doi.org/10.3389/fmolb.2021.704685

43. Eierhoff, T., Bastian, B., Thuenauer, R., Madl, J., Audfray, A., Aigal, S., … Roṁer, W. (2014). A lipid zipper triggers bacterial invasion. *Proceedings of the National Academy of Sciences of the United States of America*, *111*(35). https://doi.org/10.1073/pnas.1402637111

44. Johannes, L., & Römer, W. (2010). Shiga toxins--from cell biology to biomedical applications. *Nature reviews. Microbiology*. https://doi.org/10.1038/nrmicro2279

45. Terada, D., Voet, A. R. D., Noguchi, H., Kamata, K., Ohki, M., Addy, C., … Zhang, K. Y. J. (2017). Computational design of a symmetrical β-trefoil lectin with cancer cell binding activity. *Scientific Reports*, *7*(1). https://doi.org/10.1038/s41598-017-06332-7

46. Hasan, I., Sugawara, S., Fujii, Y., Koide, Y., Terada, D., Iimura, N., … Ozeki, Y. (2015). Mytilec, a mussel R-type lectin, interacts with surface glycan GB3 on burkitt's lymphoma cells to trigger apoptosis through multiple pathways. *Marine Drugs*. https://doi.org/10.3390/md13127071

47. Brandel, A., Aigal, S., Lagies, S., Schlimpert, M., Meléndez, A. V., Xu, M., … Römer, W. (2021). The Gb3-enriched CD59/flotillin plasma membrane domain regulates host cell invasion by Pseudomonas aeruginosa. *Cellular and Molecular Life Sciences*, *78*(7). https://doi.org/10.1007/s00018-021-03766-1

48. Lagies, S., Schlimpert, M., Neumann, S., Wäldin, A., Kammerer, B., Borner, C., & Peintner, L. (2020). Cells grown in three-dimensional spheroids mirror in vivo metabolic response of epithelial cells. *Communications Biology*, *3*(1). https://doi.org/10.1038/s42003-020-0973-6

49. Pang, Z., Chong, J., Zhou, G., De Lima Morais, D. A., Chang, L., Barrette, M., … Xia, J. (2021). MetaboAnalyst 5.0: Narrowing the gap between raw spectra and functional insights. *Nucleic Acids Research*, *49*(W1). https://doi.org/10.1093/nar/gkab382

50. Madl, J., Villringer, S., & Römer, W. (2016). Delving into Lipid-Driven Endocytic Mechanisms Using Biomimetic Membranes. https://doi.org/10.1007/8623_2016_7

51. Berg, S., Kutra, D., Kroeger, T., Straehle, C. N., Kausler, B. X., Haubold, C., Kreshuk, A. (2019). ilastik: interactive machine learning for (bio)image analysis. *Nature Methods*, *16*(12). https://doi.org/10.1038/s41592-019-0582-9

52. Zhou, D., Xu, L., Huang, W., & Tonn, T. (2018). Epitopes of MUC1 Tandem Repeats in Cancer as Revealed by Antibody Crystallography: Toward Glycopeptide Signature-Guided Therapy. *Molecules*, *23*(6), 1326. https://doi.org/10.3390/molecules23061326

53. Portoukalian, J. (2000). Immunogenity of glycolipids. *Clinical Reviews in Allergy and Immunology*. https://doi.org/10.1385/CRIAI:19:1:73

54. Imai, C., Mihara, K., Andreansky, M., Nicholson, I. C., Pui, C. H., Geiger, T. L., & Campana, D. (2004). Chimeric receptors with 4-1BB signaling capacity provoke potent cytotoxicity against acute lymphoblastic leukemia. *Leukemia*, *18*(4). https://doi.org/10.1038/sj.leu.2403302

55. Hartl, F. A., Beck-Garcìa, E., Woessner, N. M., Flachsmann, L. J., Cárdenas, R. M. H. V., Brandl, S. M., … Minguet, S. (2020). Noncanonical binding of Lck to CD3ε promotes TCR signaling and CAR function. *Nature Immunology*, *21*(8). https://doi.org/10.1038/s41590-020-0732-3

56. Maude, S. L., Barrett, D., Teachey, D. T., & Grupp, S. A. (2014). Managing cytokine release syndrome associated with novel T cell-engaging therapies. *Cancer Journal (United States)*. https://doi.org/10.1097/PPO.0000000000000035

57. Hay, K. A. (2018). Cytokine release syndrome and neurotoxicity after CD19 chimeric antigen receptor-modified (CAR-) T cell therapy. *British Journal of Haematology*. https://doi.org/10.1111/bjh.15644

58. Alam, S., Fedier, A., Kohler, R. S., & Jacob, F. (2015). Glucosylceramide synthase inhibitors differentially affect

expression of glycosphingolipids. *Glycobiology*, *25*(4), 351–356. https://doi.org/10.1093/glycob/cwu187

59. Johansson, D., Kosovac, E., Moharer, J., Ljuslinder, I., Brännström, T., Johansson, A., & Behnam-Motlagh, P. (2009). Expression of verotoxin-1 receptor Gb3 in breast cancer tissue and verotoxin-1 signal transduction to apoptosis. *BMC Cancer*, *9*. https://doi.org/10.1186/1471-2407-9-67

60. Omidvar, R., & Römer, W. (2019). Glycan-decorated protocells: Novel features for rebuilding cellular processes. *Interface Focus*. https://doi.org/10.1098/rsfs.2018.0084

61. Bhatia, T., Husen, P., Brewer, J., Bagatolli, L. A., Hansen, P. L., Ipsen, J. H., & Mouritsen, O. G. (2015). Preparing giant unilamellar vesicles (GUVs) of complex lipid mixtures on demand: Mixing small unilamellar vesicles of compositionally heterogeneous mixtures. *Biochimica et Biophysica Acta - Biomembranes*, *1848*(12). https://doi.org/10.1016/j.bbamem.2015.09.020

62. Villringer, S., Madl, J., Sych, T., Manner, C., Imberty, A., & Römer, W. (2018). Lectin-mediated protocell crosslinking to mimic cell-cell junctions and adhesion. *Scientific Reports*, *8*(1). https://doi.org/10.1038/s41598-018-20230-6

63. Schubert, T., & Römer, W. (2015). How synthetic membrane systems contribute to the understanding of lipid-driven endocytosis. *Biochimica et Biophysica Acta - Molecular Cell Research*. https://doi.org/10.1016/j.bbamcr.2015.07.014

64. Römer, W., Berland, L., Chambon, V., Gaus, K., Windschiegl, B., Tenza, D., … Johannes, L. (2007). Shiga toxin induces tubular membrane invaginations for its uptake into cells. *Nature*. https://doi.org/10.1038/nature05996

65. Pezeshkian, W., Hansen, A. G., Johannes, L., Khandelia, H., Shillcock, J. C., Kumar, P. B. S., & Ipsen, J. H. (2016). Membrane invagination induced by Shiga toxin B-subunit: From molecular structure to tube formation. *Soft Matter*, *12*(23). https://doi.org/10.1039/c6sm00464d

66. Darkow, E., Rog-Zielinska, E. A., Madl, J., Brandel, A., Siukstaite, L., Omidvar, R., … Peyronnet, R. (2020). The Lectin LecA Sensitises the Human Stretch-Activated Channel TREK-1 but Not Piezo1 and Binds Selectively to Cardiac Non-myocytes. *Frontiers in Physiology*, *11*. https://doi.org/10.3389/fphys.2020.00457

67. Posey, A. D., Schwab, R. D., Boesteanu, A. C., Steentoft, C., Mandel, U., Engels, B., … Supervision, H. S. ; (2016). Engineered CAR T Cells Targeting the Cancer-Associated Tn-Glycoform of the Membrane Mucin MUC1 Control Adenocarcinoma HHS Public Access. *Immunity*, *44*(6), 1444–1454. https://doi.org/10.1016/j.immuni

68. Kociurzynski, R., Makshakova, O. N., Knecht, V., & Römer, W. (2021). Multiscale Molecular Dynamics Studies Reveal Different Modes of Receptor Clustering by Gb3-Binding Lectins. *Journal of Chemical Theory and Computation*, *17*(4). https://doi.org/10.1021/acs.jctc.0c01145

69. Schubert, T., Sych, T., Madl, J., Xu, M., Omidvar, R., Patalag, L. J., … Römer, W. (2020). Differential recognition of lipid domains by two Gb3-binding lectins. *Scientific Reports*, *10*(1). https://doi.org/10.1038/s41598-020-66522-8

70. Steentoft, C., Migliorini, D., King, T. R., Mandel, U., June, C. H., Posey, A. D., & Freiburg, A.-L.-U. (2018). GLYCAN-DIRECTED CAR-T CELLS Running Title: Sweet CARs. https://doi.org/10.1093/glycob/cwy008/4821293

71. Chalker, J. M., Bernardes, G. J. L., Lin, Y. A., Davis, B. G., Engedal, N., Skotland, T., Franco, A. (2017). Tumor-associated antigens: Tn antigen, sTn antigen, and T antigen. *Glycobiology*, *4*(1), 157–17. https://doi.org/10.22159/ijpps.2017v9i11.2151

72. Bianchini, G., Balko, J. M., Mayer, I. A., Sanders, M. E., & Gianni, L. (2016). Triple-negative breast cancer: Challenges and opportunities of a heterogeneous disease. *Nature Reviews Clinical Oncology*. https://doi.org/10.1038/nrclinonc.2016.66

73. Durrant, L. G., Noble, P., & Spendlove, I. (2012). Immunology in the clinic review series; focus on cancer: Glycolipids as targets for tumour immunotherapy. *Clinical and Experimental Immunology*. https://doi.org/10.1111/j.1365-2249.2011.04516.x

74. Römer, W., Pontani, L. L., Sorre, B., Rentero, C., Berland, L., Chambon, V., … Johannes, L. (2010). Actin Dynamics Drive Membrane Reorganization and Scission in Clathrin-Independent Endocytosis. *Cell*, *140*(4).

https://doi.org/10.1016/j.cell.2010.01.010

75. Schütte, O. M., Ries, A., Orth, A., Patalag, L. J., Römer, W., Steinem, C., & Werz, D. B. (2014). Influence of Gb3 glycosphingolipids differing in their fatty acid chain on the phase behaviour of solid supported membranes: Chemical syntheses and impact of Shiga toxin binding. *Chemical Science*, *5*(8). https://doi.org/10.1039/c4sc01290a

76. Tavitian, B., Viel, T., Dransart, E., Nemati, F., Henry, E., Thézé, B., … Johannes, L. (2008). In vivo tumor targeting by the B-subunit of shiga toxin. *Molecular Imaging*, *7*(6). https://doi.org/10.2310/7290.2008.00022

77. Janssen, K. P., Vignjevic, D., Boisgard, R., Falguières, T., Bousquet, G., Decaudin, D., … Johannes, L. (2006). In vivo tumor targeting using a novel intestinal pathogen-based delivery approach. *Cancer Research*, *66*(14), 7230–7236. https://doi.org/10.1158/0008-5472.CAN-06-0631

78. Luginbuehl, V., Meier, N., Kovar, K., & Rohrer, J. (2018). Intracellular drug delivery: Potential usefulness of engineered Shiga toxin subunit B for targeted cancer therapy. *Biotechnology Advances*, *36*(3), 613–623. https://doi.org/10.1016/J.BIOTECHADV.2018.02.005

79. Porter, D. L., Hwang, W. T., Frey, N. V., Lacey, S. F., Shaw, P. A., Loren, A. W., … June, C. H. (2015). Chimeric antigen receptor T cells persist and induce sustained remissions in relapsed refractory chronic lymphocytic leukemia. *Science Translational Medicine*, *7*(303). https://doi.org/10.1126/scitranslmed.aac5415

80. Avigdor, A., Shouval, R., Jacoby, E., Davidson, T., Shimoni, A., Besser, M., & Nagler, A. (2018). CAR T cells induce a complete response in refractory Burkitt Lymphoma. *Bone Marrow Transplantation*. https://doi.org/10.1038/s41409-018-0235-0

81. Hill, J. A., Giralt, S., Torgerson, T. R., & Lazarus, H. M. (2019). CAR-T – and a side order of IgG, to go? – Immunoglobulin replacement in patients receiving CAR-T cell therapy. *Blood Reviews*. https://doi.org/10.1016/j.blre.2019.100596

82. Wang, Y., Cao, J., Zhiling, Y., Qiao, J., Li, D., Li, Z., & Xu, K. (2019). Kinetics of Immune Reconstitution after CD19 CAR-T Cell Therapy in ALL Patients. *Blood*, *134*(Supplement_1). https://doi.org/10.1182/blood-2019-127808

83. Yin, L., Duan, J. J., Bian, X. W., & Yu, S. C. (2020). Triple-negative breast cancer molecular subtyping and treatment progress. *Breast Cancer Research*. https://doi.org/10.1186/s13058-020-01296-5

84. Crossed D Signevenica, D., Čikeš Čulić, V., Vuica, A., & Markotić, A. (2011). Biochemical, pathological and oncological relevance of Gb3Cer receptor. *Medical Oncology*, *28*(SUPPL. 1). https://doi.org/10.1007/s12032-010-9732-8

85. Johansson, D., Andersson, C., Moharer, J., Johansson, A., & Behnam-Motlagh, P. (2010). Cisplatin-induced expression of Gb3 enables verotoxin-1 treatment of cisplatin resistance in malignant pleural mesothelioma cells. *British Journal of Cancer*, *102*(2). https://doi.org/10.1038/sj.bjc.6605467

86. Desselle, A., Chaumette, T., Gaugler, M. H., Cochonneau, D., Fleurence, J., Dubois, N., … Paris, F. (2012). Anti-Gb3 Monoclonal Antibody Inhibits Angiogenesis and Tumor Development. *PLoS ONE*, *7*(11). https://doi.org/10.1371/journal.pone.0045423

87. Salustiano, E. J., da Costa, K. M., Freire-De-Lima, L., Mendonça-Previato, L., & Previato, J. O. (2020). Inhibition of glycosphingolipid biosynthesis reverts multi-drug resistance by differentially modulating ABC transporters in chronic myeloid leukemias. *Journal of Biological Chemistry*, *295*(19). https://doi.org/10.1074/jbc.RA120.013090

88. Wu, C. P., Hsieh, C. H., & Wu, Y. S. (2011). The emergence of drug transporter-mediated multi-drug resistance to cancer chemotherapy. *Molecular Pharmaceutics*, *8*(6). https://doi.org/10.1021/mp200261n

89. Liu, Y. Y., Gupta, V., Patwardhan, G. A., Bhinge, K., Zhao, Y., Bao, J., … Jazwinski, S. M. (2010). Glucosylceramide synthase upregulates MDR1 expression in the regulation of cancer drug resistance through cSrc and β-catenin signaling. *Molecular Cancer*, *9*. https://doi.org/10.1186/1476-4598-9-145

90. Behnam-Motlagh, P., Tyler, A., Grankvist, K., & Johansson, A. (2010). Verotoxin-1 treatment or manipulation of its receptor globotriaosylceramide (Gb3) for reversal of multi-drug resistance to cancer chemotherapy. *Toxins*. https://doi.org/10.3390/toxins2102467

91. Kiarash, A., Boyd, B., & Lingwood, C. A. (1994). Glycosphingolipid receptor function is modified by fatty acid content. Verotoxin 1 and verotoxin 2c preferentially recognise different globotriaosyl ceramide fatty acid homologues. *Journal of Biological Chemistry*, *269*(15). https://doi.org/10.1016/s0021-9258(19)78102-2

92. Binnington, B., Lingwood, D., Nutikka, A., & Lingwood, C. A. (2002). Effect of globotriaosyl ceramide fatty acid α-hydroxylation on the binding by verotoxin 1 and verotoxin 2. *Neurochemical Research*, *27*(7–8). https://doi.org/10.1023/A:1020261125008

93. Lingwood, D., & Simons, K. (2010). Lipid rafts as a membrane-organising principle. *Science*. https://doi.org/10.1126/science.1174621

94. Sandvig, K., Bergan, J., Kavaliauskiene, S., & Skotland, T. (2014). Lipid requirements for entry of protein toxins into cells. *Progress in Lipid Research*. https://doi.org/10.1016/j.plipres.2014.01.001

95. Schütte, O. M., Patalag, L. J., Weber, L. M. C., Ries, A., Römer, W., Werz, D. B., & Steinem, C. (2015). 2-Hydroxy Fatty Acid Enantiomers of Gb3 Impact Shiga Toxin Binding and Membrane Organization. *Biophysical Journal*, *108*(12). https://doi.org/10.1016/j.bpj.2015.05.009

96. Rossig, C., Kailayangiri, S., Jamitzky, S., & Altvater, B. (2018). Carbohydrate targets for CAR T cells in solid childhood cancers. *Frontiers in Oncology*, *8*(NOV), 1–12. https://doi.org/10.3389/fonc.2018.00513

97. Anelli, T., & Sitia, R. (2008). Protein quality control in the early secretory pathway. *EMBO Journal*. https://doi.org/10.1038/sj.emboj.7601974

98. Muir, E., Raza, M., Ellis, C., Burnside, E., Love, F., Heller, S., … Keynes, R. (2017). Trafficking and processing of bacterial proteins by mammalian cells: Insights from chondroitinase ABC. *PLoS ONE*, *12*(11). https://doi.org/10.1371/journal.pone.0186759

99. Hamorsky, K. T., Kouokam, J. C., Jurkiewicz, J. M., Nelson, B., Moore, L. J., Husk, A. S., … Matoba, N. (2015). N-Glycosylation of cholera toxin B subunit in Nicotiana benthamiana: Impacts on host stress response, production yield and vaccine potential. *Scientific Reports*, *5*. https://doi.org/10.1038/srep08003

100. Wang, N., Wang, K. Y., Xu, F., Li, G. Q., & Liu, D. H. (2020). The effect of N-glycosylation on the expression of the tetanus toxin fragment C in Pichia pastoris. *Protein Expression and Purification*, *166*. https://doi.org/10.1016/j.pep.2019.105503

101. Amon, R., Reuven, E. M., Leviatan Ben-Arye, S., & Padler-Karavani, V. (2014). Glycans in immune recognition and response. *Carbohydrate Research*, *389*(1). https://doi.org/10.1016/j.carres.2014.02.004

102. Danishefsky, S. J., Shue, Y. K., Chang, M. N., & Wong, C. H. (2015). Development of Globo-H Cancer Vaccine. *Accounts of Chemical Research*, *48*(3). https://doi.org/10.1021/ar5004187

103. Arnaud, J., Claudinon, J., Tröndle, K., Trovaslet, M., Larson, G., Thomas, A., … Audfray, A. (2013). Reduction of lectin valency drastically changes glycolipid dynamics in membranes but not surface avidity. *ACS Chemical Biology*, *8*(9). https://doi.org/10.1021/cb400254b

104. Arnaud, J., Tröndle, K., Claudinon, J., Audfray, A., Varrot, A., Römer, W., & Imberty, A. (2014). Membrane deformation by neolectins with engineered glycolipid binding sites. *Angewandte Chemie - International Edition*. https://doi.org/10.1002/anie.201404568

Figure Captions

Fig. 1 Design of CARs and expression in primary human T cells. **a** Schematic diagram of the lentiviral vector encoding the CARs used in this study. The extracellular domain is tethered to 41BB and the T cell receptor subunit ζ. A T2A peptide sequence separates the CAR from the fluorescent protein BFP. **b-c** Surface expression of CARs and total BFP expression in primary human T cells. PBMCs were transduced with lentiviral vectors encoding CARs and expanded in the presence of IL-2 (100 U ml^{-1}). The transduction efficiency was determined by the percentage of BFP^+ cells and the presence of the FLAG-tag on the cell surface as analysed by flow cytometry. **d** Quantification of the surface expression levels of the five CARs in BFP^+ cells from three independent healthy donors. Representative data of three independent experiments are shown in b-c.

Fig 2 *In vitro* anti-tumour activity in Burkitt's lymphoma-derived cells lines induced by CAR T cells. **a** Expression of CD19 and Gb3 was assessed by staining with anti-CD19 or labelled StxB and analysed by flow cytometry. Histogram for negative control (grey), CD19 and Gb3 stained sample (dark blue). The values provided in each histogram refer to the geometric mean fluorescence intensity (MFI) and the percentage of positively stained cells. Histograms are representative of at least three independent experiments. **b** Lectin-CARs-specific killing against Burkitt's lymphoma-derived cells lines was checked by luminescence assay. Data show the percent of specific killing after 48 hours of co-incubation. **c** Kinetics of the anti-tumour activity of each lectin-CAR against Burkitt's lymphoma cell lines. One-way ANOVA followed by Dunnett's multiple comparisons test. Mean values ± s.e.m. are shown. *p< 0.05, **$p < 0.01$ ***$p < 0.001$, ****$p < 0.0001$. Data represent at least three independent donors.

Fig. 3 Activation of lectin-CAR T cells. Lectin-CAR T cells were co-incubated with $Gb3^+$ Ramos cells for 48 h. Cells were stained with anti-CD3, anti-CD8, anti-CD25 and anti-CD137 antibodies and analysed by flow cytometry. The MFI value of each subpopulation was normalised to the corresponding mock to determine the fold change. **a-c** Fold change in CD25 expression of lectin-CAR T cell subpopulations. **(a)** Total T cells, $BFP^+CD3^+CD25^+$, **(b)** cytotoxic CD8 T cells , $BFP^+CD3^+CD8^+CD25^+$, **(c)** helper CD4 T cells, $BFP^+CD3^+CD4^+CD25^+$. **d-f** Fold change in CD137 expression of lectin-CAR T cell subpopulations gated as before **(d)** total T cells, **(e)** cytotoxic CD8 T cells and (**f)** helper CD4 T cells. One way and two-way ANOVA followed by Dunnett's multiple comparisons test. Mean values ± s.e.m. are shown. n=3, simultaneously performed stimulations. *$p < 0.05$, **$p < 0.01$ ***$p < 0.001$, ****$p < 0.0001$. Representative data of one out of two independent donors.

Fig. 4 *In vitro* cell cytotoxicity and cytokine secretion by lectin-CAR T cells. **a** Kinetics of killing by BFP-sorted lectin-CAR T cells towards $Gb3^+$ $CD19^+$ Ramos and $Gb3^-$ $CD19^+$ Namalwa cell lines. Results were normalised to mock. **b-c** Amount of IFN-γ (**b**) and TNF-α (**c**) secreted by CAR T cells after 48 h of co-incubation with the indicated target cells. Effector to target (E:T) cells ratio was set to 5:1. Effector CAR T cells were BFP-sorted. Two-way ANOVA followed by Dunnett's multiple comparisons test. Mean values ± s.e.m. are shown. *$p < 0.05$, **$p < 0.01$, ***$p< 0.001$, ****$p< 0.0001$. n=3, simultaneously performed co-incubations. The data shown here were normalised to mock, as the cells were subjected to the same conditions during and after sorting. Representative data of one experiment out of two independent donors.

Fig. 5 Gb3 is specifically recognised by Shiga-CAR T cells. **a** Ramos leukaemic cells were treated as indicated and co-incubated for 24 h with effector T cells. Two-way ANOVA followed by Dunnett's multiple comparisons test. Mean values ± s.e.m. are shown, n=3, simultaneously performed co-incubation. *$p < 0.05$, **$p < 0.01$ ***$p < 0.001$, ****$p < 0.0001$, ns, not significant. Representative data of one out of two independent donors. **b** Live cell imaging of mock and Shiga-CAR T cells, which were co-incubated with giant unilamellar vesicles (GUVs) decorated with containing Gb3. Shiga-CAR T cells in green and GUVs in far-red. GUVs were composed of DOPC, cholesterol, DOPE and Gb3 (59.7: 30: 0.3: 10 mol%, respectively). Images from selected areas were monitored. Zoom areas are marked with a white frame, and the arrow indicates membrane bending. Scale bars 20 μm **c** The contact of Shiga-CAR T cells or mock t cells and GUVs is displayed as percent. Quantified green, red and co-localised pixels were used to calculate the percent of contact. Lines represent median values of the percent of contact in the monitored areas over time.

Fig. 6 *In vitro* solid tumour cell killing by CAR T cells. **a** Expression of Gb3 was assessed by staining with 647-labelled StxB and flow cytometry. **b** Lectin-CAR specific killing of colorectal cancer cell lines (HT-29, HTC-116, LS-174) and breast cancer cell lines (MDA-MB-231 and JIMT1) was checked by bioluminescence assay at 48 h. One-way ANOVA followed by Dunnett's multiple comparisons test. Mean values ± s.e.m. are shown. Data represent at least three independent experiments. *$p < 0.05$, **$p < 0.01$, ***$p < 0.001$, ****$p < 0.0001$. **c** Kinetics of the killing of each lectin-CAR against solid

tumour cell lines. Mean values ± s.e.m. are shown. Data represent at least three independent experiments. **d** Killing kinetics of BFP-sorted lectin-CAR T cells. Mean values ± s.e.m. are shown. n=3, simultaneously performed co-incubation. Mock was considered for normalisation. Representative experiment out of two independent donors.

Fig. 7 Lipid analysis by MS reveals Gb3 abundance and dominant isoforms present in the studied cell lines. **a** Total Gb3 content per cell line. **b** Distribution of Gb3 isoforms in HT-29 cells. Most common present Gb3 isoforms were (d18:1/C16:0-OH), (d18:1/C16:0) and (d18:1/C24:0). **c** Distribution of Gb3 isoforms in Ramos cells. Most abundant Gb3 isoforms were (d18:1/C24:1), (d18:1/C16:0) and (d18:1/C24:0). **d** Distribution of Gb3 isoforms in MDA-MB-231 cells. Dominantly present species were (d18:1/C24:0), (d18:1/C24:1) and (d18:1/C16:0). Displayed Gb3 species were normalised to an internal standard and the sum of all detected sphingolipid. Mean values ± s.e.m. are shown. n=3, analysed samples in one LC-MS sequence. **e** Heat map of Pearson's correlation coefficient of the Gb3 isoform abundance and the specific killing by lectin-CAR T cells.

Figures

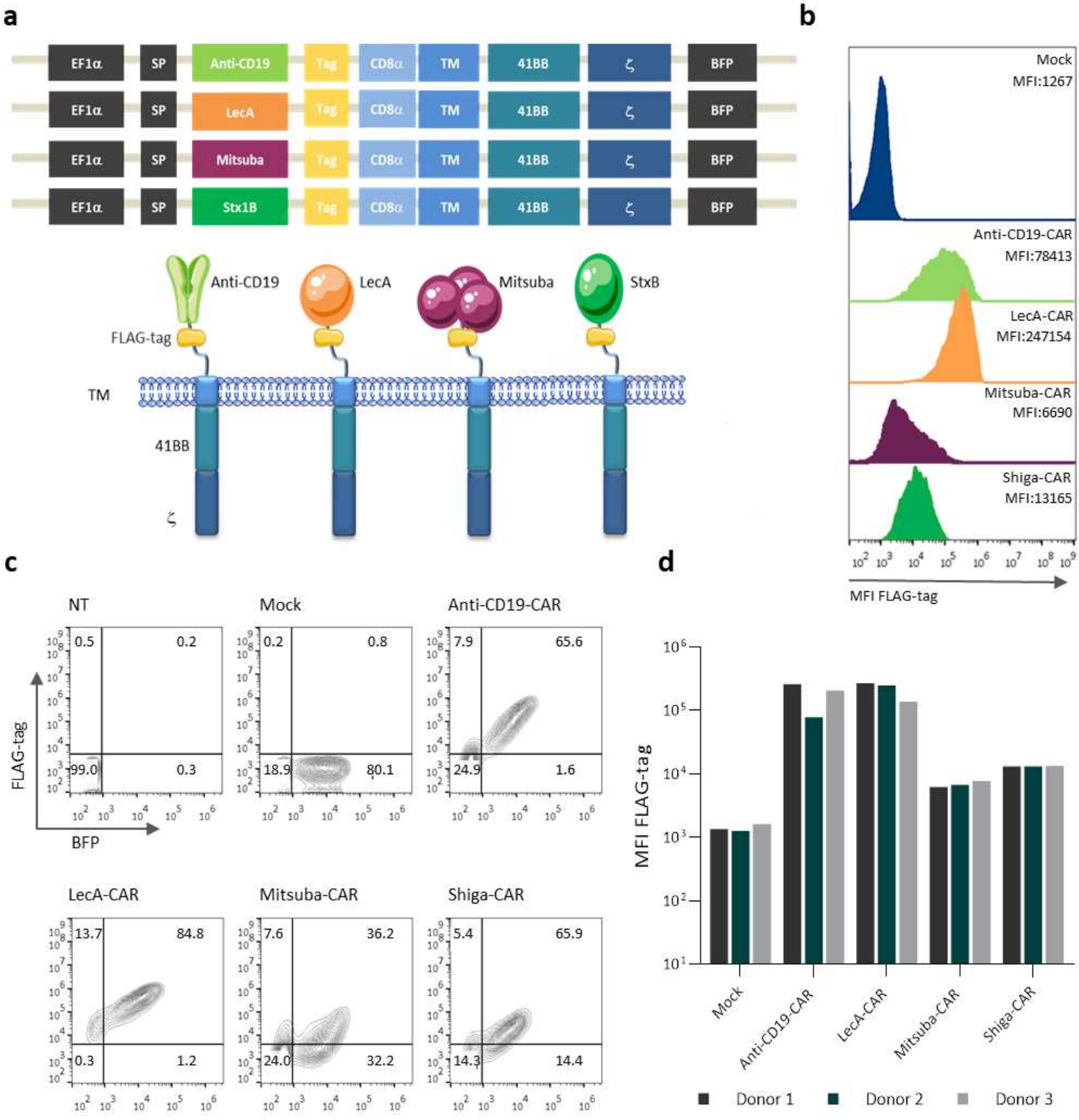

Figure 1

Design of CARs and expression in primary human T cells. a Schematic diagram of the lentiviral vector encoding the CARs used in this study. The extracellular domain is tethered to 41BB and the T cell receptor subunit ζ . A T2A peptide sequence separates the CAR from the fluorescent protein BFP. b-c Surface

expression of CARs and total BFP expression in primary human T cells. PBMCs were transduced with lentiviral vectors encoding CARs and expanded in the presence of IL-2 (100 U ml-1). The transduction efficiency was determined by the percentage of BFP cells and the presence of the FLAG-tag on the cell surface as analysed by flow cytometry. d Quantification of the surface expression levels of the five CARs in BFP cells from three independent healthy donors. Representative data of three independent experiments are shown in b-c.

Figure 2

In vitro anti-tumour activity in Burkitt's lymphoma-derived cells lines induced by CAR T cells. a Expression of CD19 and Gb3 was assessed by staining with anti-CD19 or labelled StxB and analysed by flow cytometry. Histogram for negative control (grey), CD19 and Gb3 stained sample (dark blue). The values provided in each histogram refer to the geometric mean fluorescence intensity (MFI) and the percentage of positively stained cells. Histograms are representative of at least three independent experiments. b Lectin-CARs-specific killing against Burkitt's lymphoma-derived cells lines was checked by luminescence assay. Data show the percent of specific killing after 48 hours of co-incubation. c Kinetics of the anti-tumour activity of each lectin-CAR against Burkitt's lymphoma cell lines. One-way ANOVA followed by Dunnett's multiple comparisons test. Mean values ± s.e.m. are shown. *p< 0.05, **p < 0.01 ***p < 0.001, ****p < 0.0001. Data represent at least three independent donors.

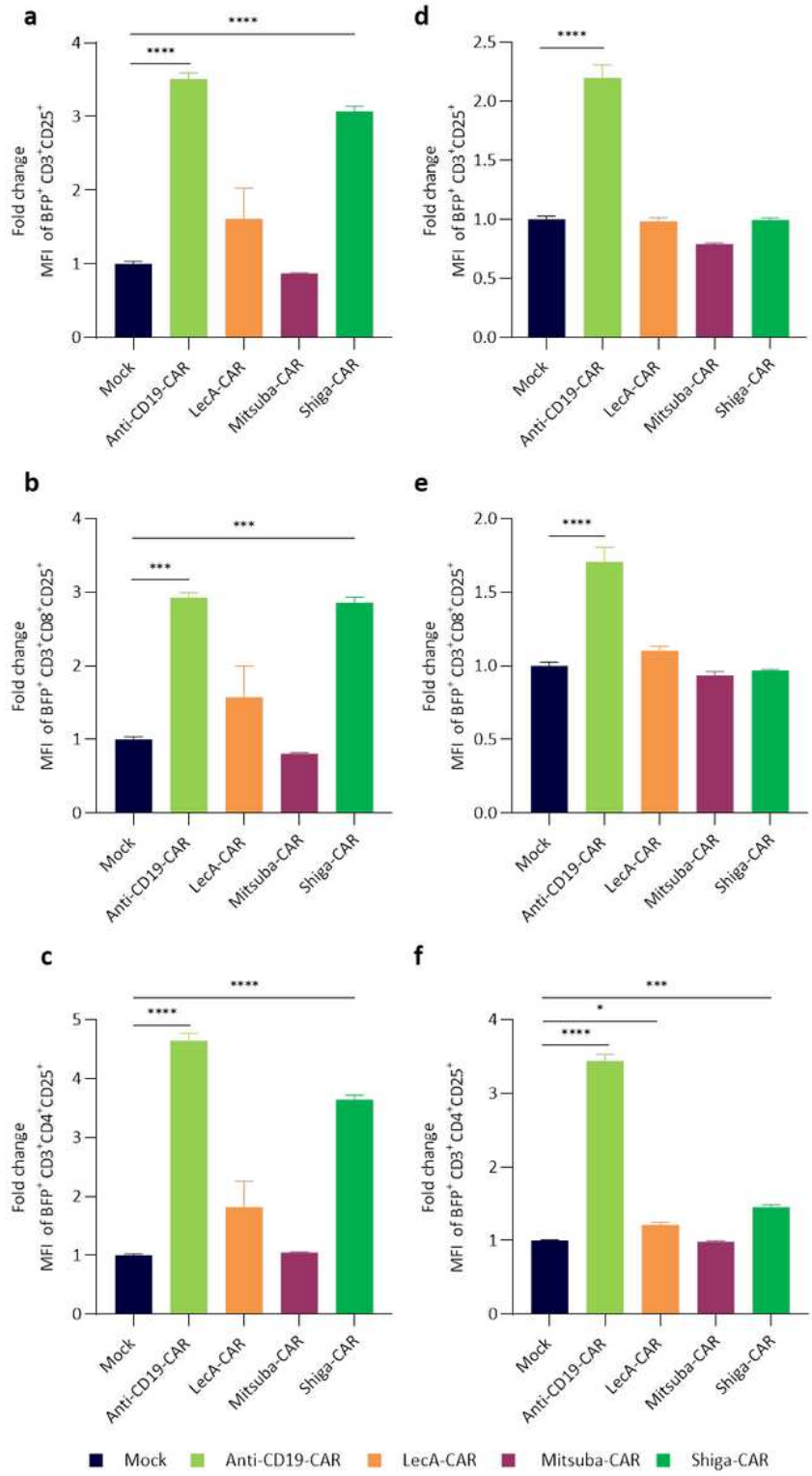

Figure 3

Activation of lectin-CAR T cells. Lectin-CAR T cells were co-incubated with Gb3⁺ Ramos cells for 48 h. Cells were stained with anti-CD3, anti-CD8, anti-CD25 and anti-CD137 antibodies and analysed by flow cytometry. The MFI value of each subpopulation was normalised to the corresponding mock to determine the fold change. a-c Fold change in CD25 expression of lectin-CAR T cell subpopulations. (a) Total T cells, BFP⁺CD3⁺CD25⁺, (b) cytotoxic CD8 T cells , BFP⁺CD3⁺CD8⁺CD25⁺, (c) helper CD4 T cells,

BFP⁺CD3⁺CD4⁺CD25⁺. d-f Fold change in CD137 expression of lectin-CAR T cell subpopulations gated as before (d) total T cells, (e) cytotoxic CD8 T cells and (f) helper CD4 T cells. One way and two-way ANOVA followed by Dunnett's multiple comparisons test. Mean values ± s.e.m. are shown. n=3, simultaneously performed stimulations. *p < 0.05, **p < 0.01 ***p < 0.001, ****p < 0.0001. Representative data of one out of two independent donors.

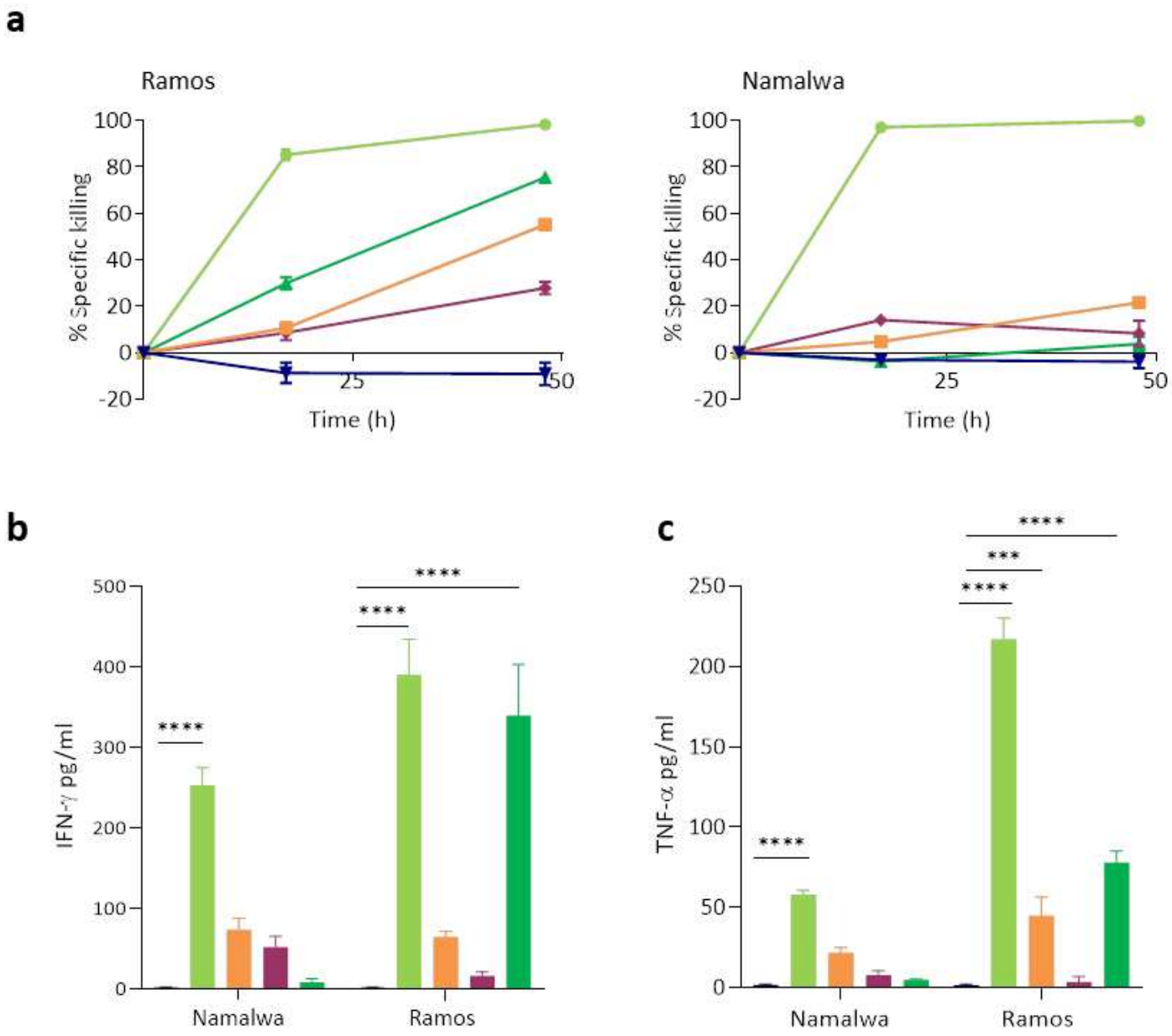

Figure 4

In vitro cell cytotoxicity and cytokine secretion by lectin-CAR T cells. a Kinetics of killing by BFP-sorted lectin-CAR T cells towards Gb3⁺ CD19⁺ Ramos and Gb3⁺ CD19⁺ Namalwa cell lines. Results were normalised to mock. b-c Amount of IFN-γ(b) and TNF-α (c) secreted by CAR T cells after 48 h of co-incubation with the indicated target cells. Effector to target (E:T) cells ratio was set to 5:1. Effector CAR T cells were BFP-sorted. Two-way ANOVA followed by Dunnett's multiple comparisons test. Mean values ±

s.e.m. are shown. *p < 0.05, **p < 0.01, ***p< 0.001, ****p< 0.0001. n=3, simultaneously performed co-incubations. The data shown here were normalised to mock, as the cells were subjected to the same conditions during and after sorting. Representative data of one experiment out of two independent donors.

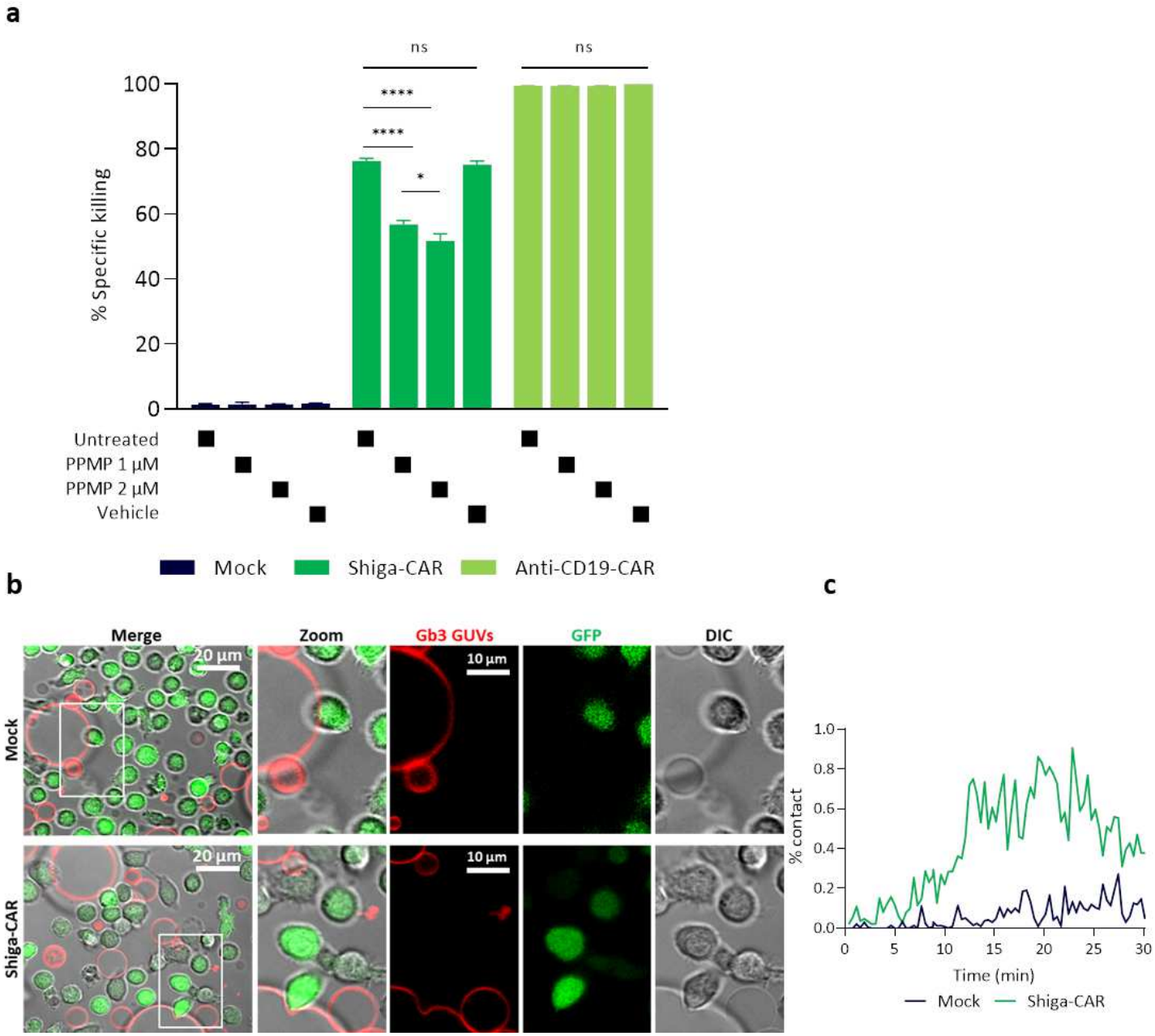

Figure 5

Gb3 is specifically recognised by Shiga-CAR T cells. a Ramos leukaemic cells were treated as indicated and co-incubated for 24 h with effector T cells. Two-way ANOVA followed by Dunnett's multiple comparisons test. Mean values ± s.e.m. are shown, n=3, simultaneously performed co-incubation. *p < 0.05, **p < 0.01 ***p < 0.001, ****p < 0.0001, ns, not significant. Representative data of one out of two independent donors. b Live cell imaging of mock and Shiga-CAR T cells, which were co-incubated with

giant unilamellar vesicles (GUVs) decorated with containing Gb3. Shiga-CAR T cells in green and GUVs in far-red. GUVs were composed of DOPC, cholesterol, DOPE and Gb3 (59.7: 30: 0.3: 10 mol%, respectively). Images from selected areas were monitored. Zoom areas are marked with a white frame, and the arrow indicates membrane bending. Scale bars 20 µm c The contact of Shiga-CAR T cells or mock t cells and GUVs is displayed as percent. Quantified green, red and co-localised pixels were used to calculate the percent of contact. Lines represent median values of the percent of contact in the monitored areas over time.

Figure 6

In vitro solid tumour cell killing by CAR T cells. a Expression of Gb3 was assessed by staining with 647-labelled StxB and flow cytometry. b Lectin-CAR specific killing of colorectal cancer cell lines (HT-29, HTC-116, LS-174) and breast cancer cell lines (MDA-MB-231 and JIMT1) was checked by bioluminescence assay at 48 h. One-way ANOVA followed by Dunnett's multiple comparisons test. Mean values ± s.e.m. are shown. Data represent at least three independent experiments. *p < 0.05, **p < 0.01, ***p < 0.001, ****p < 0.0001. c Kinetics of the killing of each lectin-CAR against solid

tumour cell lines. Mean values ± s.e.m. are shown. Data represent at least three independent experiments. d Killing kinetics of BFP-sorted lectin-CAR T cells. Mean values ± s.e.m. are shown. n=3, simultaneously performed co-incubation. Mock was considered for normalisation. Representative experiment out of two independent donors.

Figure 7

Lipid analysis by MS reveals Gb3 abundance and dominant isoforms present in the studied cell lines. a Total Gb3 content per cell line. b Distribution of Gb3 isoforms in HT-29 cells. Most common present Gb3 isoforms were (d18:1/C16:0-OH), (d18:1/C16:0) and (d18:1/C24:0). c Distribution of Gb3 isoforms in Ramos cells. Most abundant Gb3 isoforms were (d18:1/C24:1), (d18:1/C16:0) and (d18:1/C24:0). d Distribution of Gb3 isoforms in MDA-MB-231 cells. Dominantly present species were (d18:1/C24:0), (d18:1/C24:1) and (d18:1/C16:0). Displayed Gb3 species were normalised to an internal standard and the sum of all detected sphingolipid. Mean values ± s.e.m. are shown. n=3, analysed samples in one LC-MS sequence. e Heat map of Pearson's correlation coefficient of the Gb3 isoform abundance and the specific killing by lectin-CAR T cells.

Supplementary Files

This is a list of supplementary files associated with this preprint. Click to download.

- OnlineResource1.avi
- Supplementaryfile1.pdf
- Supplementaryfile2.pdf
- OnlineResource2.avi